



Optimization of a flexible multi-generation system based on wood chip gasification and methanol production

Lythcke-Jørgensen, Christoffer Ernst; Clausen, Lasse Røngaard; Algren, Loui ; Bavnhøj Hansen, Anders; Münster, Marie; Gadsbøll, Rasmus Østergaard; Haglind, Fredrik

Published in:
Applied Energy

Link to article, DOI:
[10.1016/j.apenergy.2016.08.092](https://doi.org/10.1016/j.apenergy.2016.08.092)

Publication date:
2017

Document Version
Peer reviewed version

[Link back to DTU Orbit](#)

Citation (APA):
Lythcke-Jørgensen, C. E., Clausen, L. R., Algren, L., Bavnhøj Hansen, A., Münster, M., Gadsbøll, R. Ø., & Haglind, F. (2017). Optimization of a flexible multi-generation system based on wood chip gasification and methanol production. *Applied Energy*, 192, 337–359. <https://doi.org/10.1016/j.apenergy.2016.08.092>

General rights

Copyright and moral rights for the publications made accessible in the public portal are retained by the authors and/or other copyright owners and it is a condition of accessing publications that users recognise and abide by the legal requirements associated with these rights.

- Users may download and print one copy of any publication from the public portal for the purpose of private study or research.
- You may not further distribute the material or use it for any profit-making activity or commercial gain
- You may freely distribute the URL identifying the publication in the public portal

If you believe that this document breaches copyright please contact us providing details, and we will remove access to the work immediately and investigate your claim.

1 Optimization of a flexible multi-generation 2 system based on wood chip gasification and 3 methanol production

4 *Christoffer Lythcke-Jørgensen*^{a*}, *Lasse Røngaard Clausen*^a, *Loui Algren*^b, *Anders Bavnhøj Hansen*^b, *Marie*
5 *Münster*^c, *Rasmus Østergaard Gadsbøll*^d, *Fredrik Haglind*^a

6 ^a *Technical University of Denmark, Department of Mechanical Engineering*

7 ^b *Energinet.dk*

8 ^c *Technical University of Denmark, Department of Management Engineering*

9 ^d *Technical University of Denmark, Department of Chemical and Biochemical Engineering*

10 * *Corresponding author. Email: celjo@mek.dtu.dk. Phone: +45 30 42 72 00. Nils Koppels Allé 403, 2800 Kgs.*
11 *Lyngby, Denmark.*

12 **Abstract**

13 Flexible multi-generation systems (FMGs) consist of integrated and flexibly operated facilities that provide
14 multiple links between the different sectors of the energy system. The present study treated the design
15 optimization of a conceptual FMG which integrated a methanol-producing biorefinery with an existing
16 combined heat and power (CHP) unit and industrial energy utility supply in the Danish city of Horsens. The
17 objective was to optimize economic performance and minimize total CO₂ emission of the FMG which was
18 required to meet the local district heating demand plus the thermal utility demand of the butchery. The
19 design optimization considered: Selection, dimensioning, location and integration of processes; operation
20 optimization with respect to both hourly variations in operating conditions over the year as well as
21 expected long term energy system development; and uncertainty analysis considering both investment
22 costs and operating conditions.

23 Applying a previously developed FMG design methodology, scalable models of the considered processes
24 were developed and the system design was optimized with respect to hourly operation over the period
25 2015-2035. The optimal design with respect to both economic and environmental performance involved a
26 maximum-sized biorefinery located next to local industry rather than in connection with the existing CHP
27 unit. As the local industry energy demands were limited when compared to the biorefinery dimensions
28 considered, process integration synergies were found to be marginal when compared to the economic and
29 environmental impact of the biorefinery for the present case.

30 Assessing the impact of uncertainties on the estimated FMG performances, the net present value (NPV) of
31 the optimal design was estimated to vary within the range 252.5 M€ to 1471.6 M€ in response to changes
32 of $\pm 25\%$ in investment costs and methanol price, and considering two different electricity price scenarios.
33 In addition, a change in the interest rate from 5% to 20% was found to reduce the lower bound of the NPV
34 to 181.3 M€ for reference operating conditions. The results suggest that the applied interest rate and
35 operating conditions, in particular the methanol price, would have a much higher impact on the economic
36 performance of the designs than corresponding uncertainties in investment costs. In addition, the study

37 outcomes emphasize the importance of including systematic uncertainty analysis in the design optimization
38 of FMG concepts.

39 **Keywords:** Biomass gasification, design optimization, flexible multi-generation, polygeneration, process
40 integration, smart energy systems

41 **Nomenclature**

42 **Latin letters**

43	C_0	Net present value	[M€]
44	$C_{inv,k}$	Investment cost, process k	[M€]
45	$C_{inv,k0}$	Reference investment cost, process k	[M€]
46	$c_{op,i}$	Hourly operation result	[M€/h]
47	$c_{op,k}$	Operation cost, process k	[M€/h]
48	p_f	Power factor for economy-of-scale calculations	[-]
49	r	Interest rate	[-]
50	T	Number of years from installation date	[-]
51	t_i	Duration of period i	[h]
52	$t_{PV,i}$	Present value factor of period i	[h]
53	Z_0	Total CO ₂ emission impact	[MTon]
54	z_{op}	Hourly CO ₂ emission impact of operation	[MTon]

55 **Greek letters**

56	σ	Process dimension
57	ω	Installation decision (integer)
58	λ	Load

59 **Subscripts**

60	i	Period
61	k	Process

62 **Abbreviations**

63	CCHP	Combined cooling, heat and power
64	CHOP	Characteristic operating pattern
65	CHP	Combined heat and power
66	FMG	Flexible multi-generation systems
67	NPV	Net present value
68	RES	Renewable energy sources
69	SOEC	Solid oxide electrolysis cell
70	TCE	Total CO ₂ emission impact

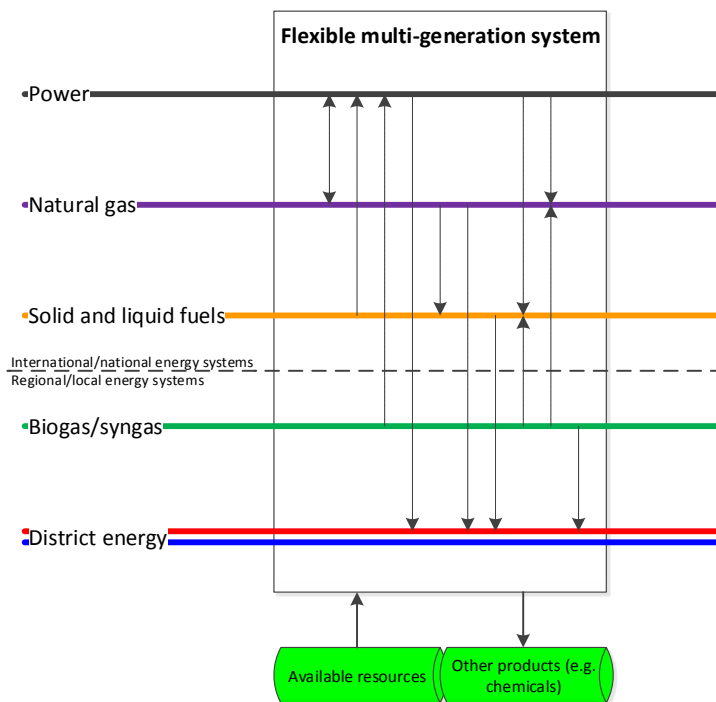
71

72 **1. Introduction**

73 The transition towards sustainable energy systems based on intermittent renewable energy sources (RES)
74 necessitates the development of efficient means for balancing generation and consumption of energy
75 services. While focus previously was centred on developing smart grid technology for the power grid,
76 recent studies suggests that the challenge of balancing generation from renewables is better appreciated
77 from a holistic energy system perspective in order to avoid suboptimal, sector-based solutions [1][2]. This
78 holistic approach has been referred to as a Smart Energy System approach, and it promotes the integration
79 of power, thermal and gas grids, and the use of various energy storage options in combination in order to
80 achieve secure and sustainable energy systems based on renewable sources [3].

81 However, synergies from integrating energy conversion process in multi-generation systems are not
82 considered directly using the smart energy systems approach. These synergies may be of great importance
83 in the transition towards sustainable energy systems [4], especially regarding biomass conversion where it
84 has been suggested that systematic consideration of process integration synergies may increase the
85 energy- and cost-efficiency of the conversion as well as the overall system [5].

86 Responding to this, the concept of flexible multi-generation systems (FMG) was recently introduced by
87 Lythcke-Jørgensen et al. [6]. Here, FMGs were defined as integrated systems that generate multiple energy
88 services and are able to adjust operation in response to fluctuating demand patterns and varying price
89 schemes in the overarching energy system. The hypothesis is that local or regional FMGs may support the
90 balancing of an energy system with large shares of variable RES in a cost-effective way by linking the
91 different parts of the energy system with local supply systems. By converting energy in response to demand
92 and price variations, FMGs may be regarded as virtual energy system valves as conceptually illustrated in
93 Figure 1, making the development of FMGs a relevant topic.



94

95 **Figure 1: Conceptual sketch of the FMG concept [6]. Dotted arrows indicate a range of technological pathways for linking the**
96 **energy system layers in an FMG.**

97 The development of FMGs is complex and involves multiple design aspects. Within these, five aspects are
98 considered of special relevance:

- 99 1. Process selection and dimensioning
- 100 2. Systematic process integration
- 101 3. Variable short-term operation conditions, including hourly, diurnal, weekly and seasonal changes in
102 demands and generation from variable RES
- 103 4. Variable long-term operation conditions, responding to developments in the energy system
- 104 5. Uncertainty analysis

105 Numerous approaches for designing multi-generation systems have been presented in literature [7,8], but
106 as discussed in Lythcke-Jørgensen et al. [6], none of these are able to consider all five listed aspects
107 coherently. For instance, Liu et al. [9] developed a stochastic, multi-objective mixed integer-nonlinear
108 programming model for designing polygeneration¹ systems based on several previous works, but did not
109 consider short-term operation or process integration. Based on the OSMOSE tool², Maréchal et al. [10]
110 presented a multi-period, multi-objective methodology for designing multi-generation systems which
111 considered technology selection and dimensioning, process integration, selection of facility location
112 selection, flexible operation, and network layout. Fazlollahi et al. developed three add-ons to the
113 methodology to allow for the structured reduction of operation periods [11], inclusion of daily thermal
114 storages [12] and detailed design of distribution networks [13]. However, the combined methodology only
115 considered variations in one external operating condition, namely outdoor temperature, meaning that
116 flexible interactions with other parts of the energy system were not considered. In addition, uncertainties
117 were not addressed in the combined methodology. In consequence, a novel methodology for designing
118 FMGs was introduced in Lythcke-Jørgensen et al. [6] which included all the listed aspects as well as others,
119 including biomass supply chains.

120 A number of specific FMG concepts have been treated in case studies. Regarding FMGs integrating the heat
121 and power layers, Lund et al. [2] presented the case of Skagen combined heat and power (CHP) plant which
122 included three CHP units, thermal energy storage, a peak load gas boiler, and an electrical boiler. The
123 system effectively created a dual link between the electricity grid and the district heating system as the
124 plant was able to both generate electricity and heat directly as well as convert electricity to heat. In a study
125 of a comparable system, Sorknæs et al. [14] found that the system's ability of provide electricity grid
126 balancing could increase the overall CHP operation load by 25% and reduce net heat production costs by
127 5% for a specific heating network. However, it was questioned if the results would be valid in case multiple
128 comparable systems adopted a similar operation strategy due to the limited size of the balancing market. In
129 two closely related works, Capuder and Mancarella [15][16] studied seven different schemes for supplying
130 electricity and heating in the UK. In a study, the group found that FMG schemes consisting of CHP units,
131 electric heat pumps, and thermal energy storage may reduce investment and operating costs as well as
132 aggregate emission levels when compared to conventional or less flexible heat-and-electricity supply

¹ In a recent review, Adams and Ghouse [52] defined 'polygeneration' as a thermochemical process which simultaneously generates electricity and produces at least one type of chemical or fuel without being a co- or tri-generation unit

² OSMOSE is a computer aided process engineering tool, developed at EPFL in the IPESE group, for designing and optimizing integrated energy systems. For more information, refer to [46] or the IPESE group homepage: <http://ipese.epfl.ch/>.

133 systems in the UK. The group further found that FMG schemes may allow for reductions in both expected
134 costs and risks under long-term price uncertainty scenarios when compared to less flexible systems [17].

135 Another branch of FMGs integrate the power, heating and cooling layers and are also referred to as
136 combined cooling, heating and power (CCHP) systems. Piacentino et al. [18] introduced a methodology for
137 maximizing the net present value (NPV) of CCHP systems for building clusters by considering component
138 selection, dimensioning, and operation optimization with respect to hourly energy demands. Zhou et al.
139 [19] presented a methodology for designing distributed CCHP systems based on a two-stage stochastic
140 programming model which accounted for selection, dimensioning, and operation optimization of
141 combinations of equipment under uncertain operating conditions. Rubio-Maya et al. [20] presented a
142 heuristic, two-level methodology for designing local FMGs for CCHP and fresh water generation and in a
143 case study found that an integrated natural-gas based scheme would be profitable when compared to a
144 stand-alone solution.

145 Among FMGs integrating the power grid and liquid fuel layer, Chen et al. [21] studied an FMG using coal
146 and biomass to generate electricity and co-produce naphtha, diesel and methanol. The group found that
147 flexible systems in general achieved higher NPVs than static systems, however at the cost of larger
148 investments. In three related works, Lythcke-Jørgensen et al. [22–24] studied an FMG concept integrating
149 cellulosic ethanol production with a CHP unit, creating a virtual link between the electricity, heating and
150 fuel systems. Models and process integration strategies were analysed and optimized, and it was found
151 that the lack of flexibility in the ethanol production induced inefficient operation during periods with high
152 electricity prices, causing the entire system to be economically uncompetitive in an energy system with a
153 large share of wind power [22]. At the same time, the average exergy efficiency of the ethanol production
154 was markedly reduced when compared to the exergy efficiency in optimal operation [23]. It was further
155 found that a diseconomy-of-scale trend applied for the ethanol production in the FMG under the set
156 conditions as reductions in integration synergies exceeded the benefits from economy-of-scale in
157 investment and operating costs [24]. These outcomes illustrate some of the challenges faced when
158 developing flexible technologies for energy systems with large shares of varying RES.

159 In two recent studies, Lythcke-Jørgensen et al. [6,25] studied an FMG concept combining heat and power
160 generation with the production of cellulosic ethanol and biogas-based synthetic natural gas. It was
161 demonstrated how operation flexibility is a central aspect when assessing the performance of FMGs [25],
162 and that systematic process integration ought to be considered when optimizing the design of FMGs [6].
163 The outcomes illustrate the importance of systematically considering the five previously listed design
164 aspects when developing FMGs.

165 This paper treats the development of a conceptual FMG based on an existing CHP unit and local industry.
166 The FMG was developed for producing methanol from biomass and supplying district heating and industrial
167 energy utilities. Using the state-of-the-art design optimization methodology presented in Lythcke-
168 Jørgensen et al. [6], the FMG was optimized with the aim of maximizing NPV and minimizing the total CO₂
169 emission impact (TCE) from operating the system over the period 2015-2035. Technologies considered
170 include a two-stage biomass gasifier, a solid oxide electrolysis cell (SOEC), a methanol production facility,
171 industrial heat pumps, and novel heat and gas infrastructures, altogether linking the power, district heating,
172 natural gas, and fuel layers of the energy system.

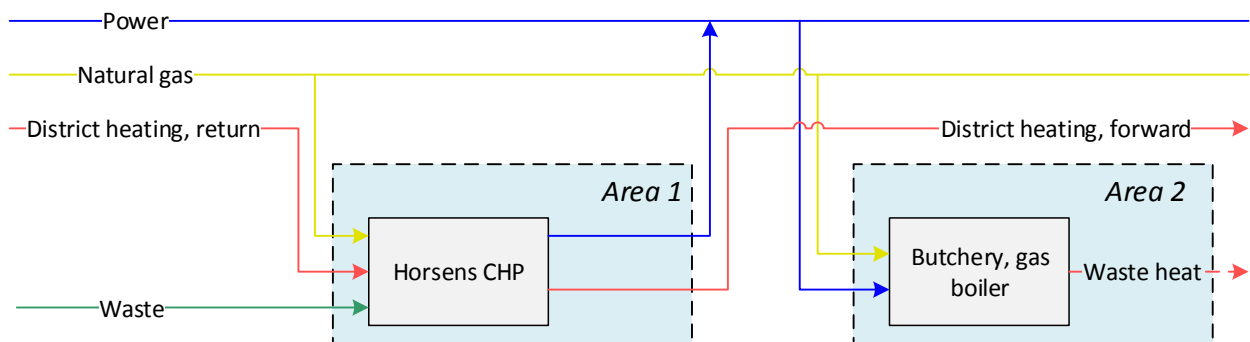
173 The present work addresses the knowledge gap between process level optimization and energy system
174 optimization by taking system level variations into account when designing energy conversion systems. The
175 novelty of the study lies in the design optimization that coherently considers: Process selection and
176 dimensioning; systematic process integration using pinch analysis; consideration of local demands for
177 energy services and local infrastructures; performance assessment with respect to hourly variations in
178 operating conditions as well as long-term energy system development; and uncertainty analysis considering
179 uncertainties in important design parameters. In addition, the design optimization assesses performance
180 variations with respect to various energy system scenarios and applied interest rate in the NPV calculation.
181 To the authors' best knowledge, no previous work has presented such comprehensive approach to the
182 design optimization of an FMG concept.

183 In this paper, the case study considered and the applied optimization methodology are described in Section
184 2. Results of the design optimization and systematic assessment of uncertainties are presented in Section 3,
185 while Section 4 features a discussion on potential drawbacks of the work and recommendations for future
186 research within this field. A conclusion on the study is presented in Section 5. Appendix A features a full
187 documentation of the process modelling, while Appendix B includes documentation on the structuring of
188 energy system scenario datasets in the present work.

189 2. Methods

190 2.1. Case description

191 The case study treated in this paper was centred on the Horsens Kraftvarmeværk, a back-pressure CHP unit
192 in the Danish city of Horsens with a population of 56,536 [26]. The back-pressure CHP unit has a full-load
193 capacity of 7 MWe and 25 MJ/s district heating and consists of a steam Rankine cycle with two 5 ton/hour
194 waste incineration boilers. In addition, a gas turbine is installed on site, which is capable of boosting district
195 heating production with 8 MJ/s [27]. Furthermore, a large butchery located approximately 9 km from the
196 CHP unit was included in the case study. The thermal utility demand of the butchery was assumed covered
197 by natural gas in the reference case. A sketch of the reference system is presented in Figure 2.

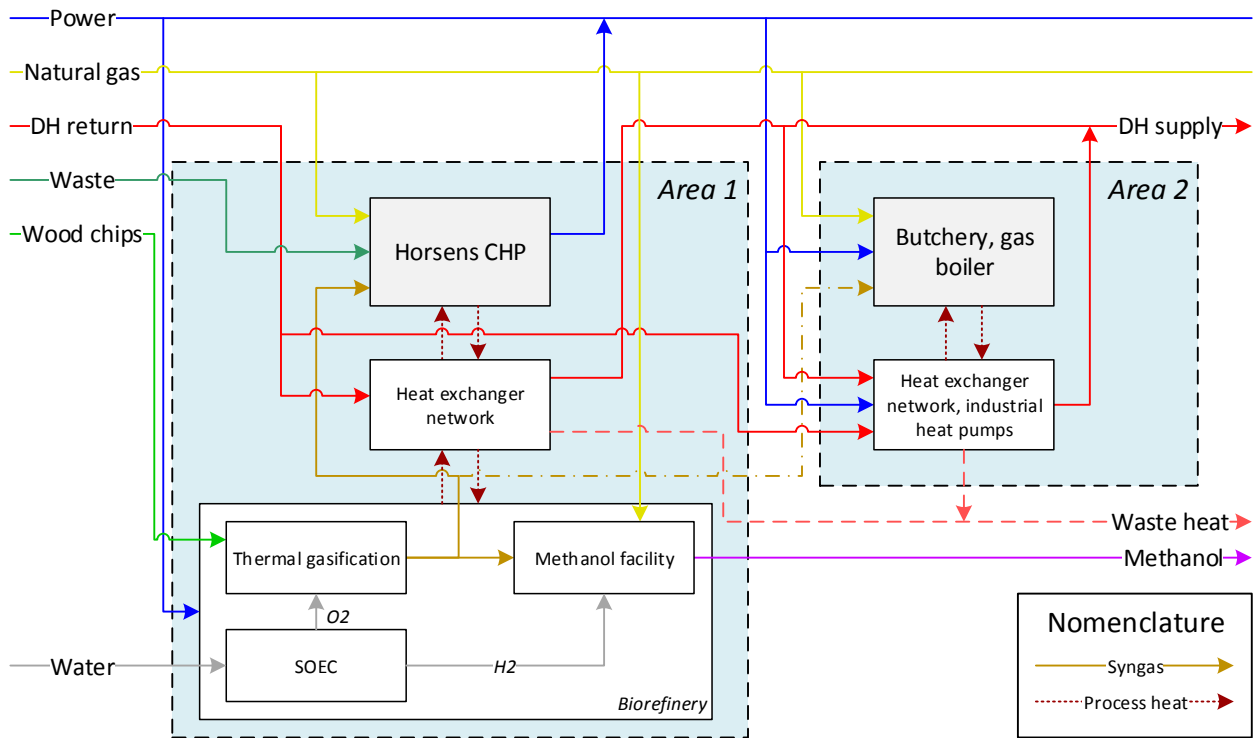


198
199 **Figure 2: Conceptual sketch of energy flows in the reference system.**

200 The case study treated the retrofitting of the reference system by installing a biorefinery, consisting of a
201 two-stage biomass gasifier [28], a solid oxide electrolysis cell (SOEC), and a methanol production facility.
202 The biorefinery was to be installed either next to the CHP unit or the butchery, and the installation of a
203 product gas pipeline between the two areas was considered. In addition, investment in a district heating

204 link to the butchery area was considered in order to cover parts of the butchery thermal utility demands
 205 through district heating using ammonia-water hybrid heat pumps. The conceptual retrofit options are
 206 illustrated in Figures 3 and 4.

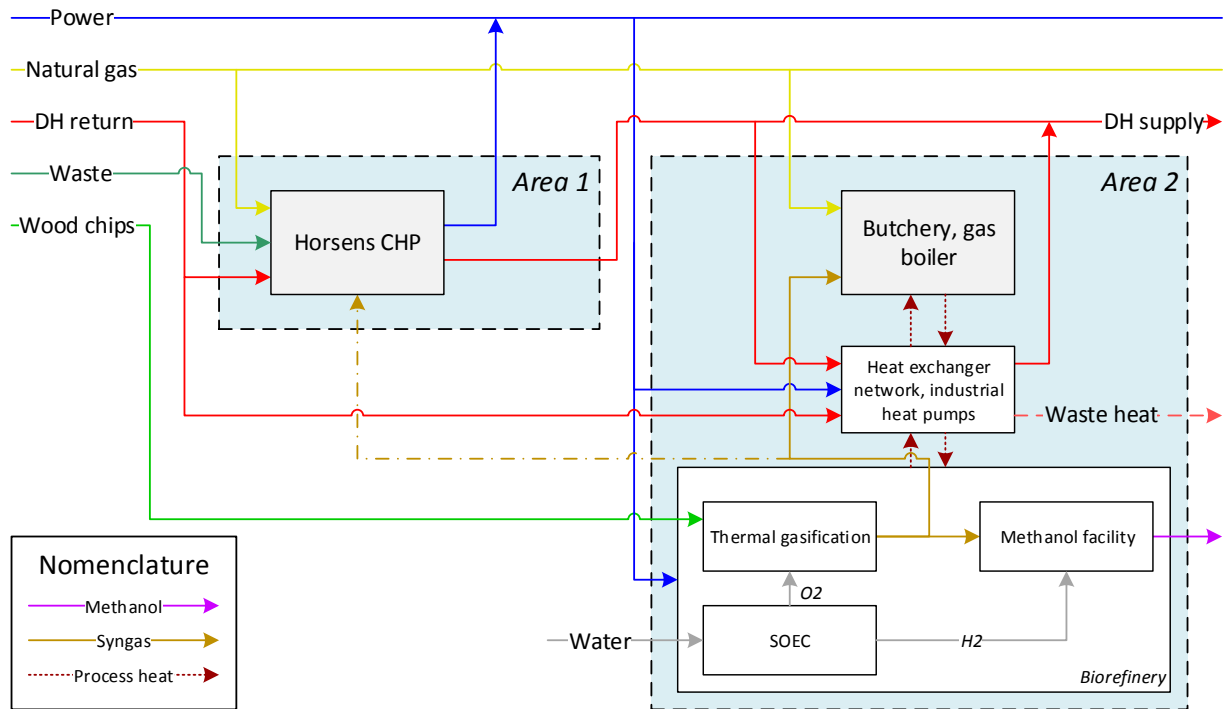
207 The hypothesis is that the present FMG is advantageous in an energy system with large shares of
 208 intermittent renewable power generation as it may absorb additional power in periods with excess
 209 generation (low power prices) and convert it to methanol by boosting product gas from the gasifier with
 210 hydrogen from the SOEC [29]. Similarly, it may reduce power consumption in periods with high power
 211 prices by reducing SOEC load and thereby methanol production. At the same time, process integration is
 212 used to optimize the overall energy conversion efficiency of the system, potentially increasing
 213 thermodynamic and economic efficiencies when compared to non-integrated facilities [6,25]. Process heat
 214 demands of the butchery could further be met through process integration with the biorefinery, by
 215 compression-based ammonia-water hybrid heat pumps using district heating as heat source, or by product
 216 gas combusted in the butchery gas boiler. In addition, non-reacted product gas may replace parts of the gas
 217 utility demand of the butchery, thereby replacing natural gas. In total, this tentative combination of
 218 processes allows for a flexible energy supply system capable of converting biomass resources to demanded
 219 energy services in order to replace fossil fuels while at the same time providing links between the electricity,
 220 district heating, natural gas, and fuel sectors of the overarching energy system.



221

222 **Figure 3: Conceptual sketch of energy flows in 'Retrofit Scenario A' with the biorefinery installed next to the CHP unit. Notice**
 223 **that the process heat flows represent feasible heat integration options between the facilities. Process integration options within**
 224 **the facilities are not illustrated in the figure for simplicity.**

225



226

227 **Figure 4: Conceptual sketch of energy flows in 'Retrofit Scenario B' with the biorefinery installed next to the butchery. Notice**
228 **that the process heat flows represent feasible heat integration options between the facilities. Process integration options within**
229 **the facilities are not illustrated in the figure for simplicity.**

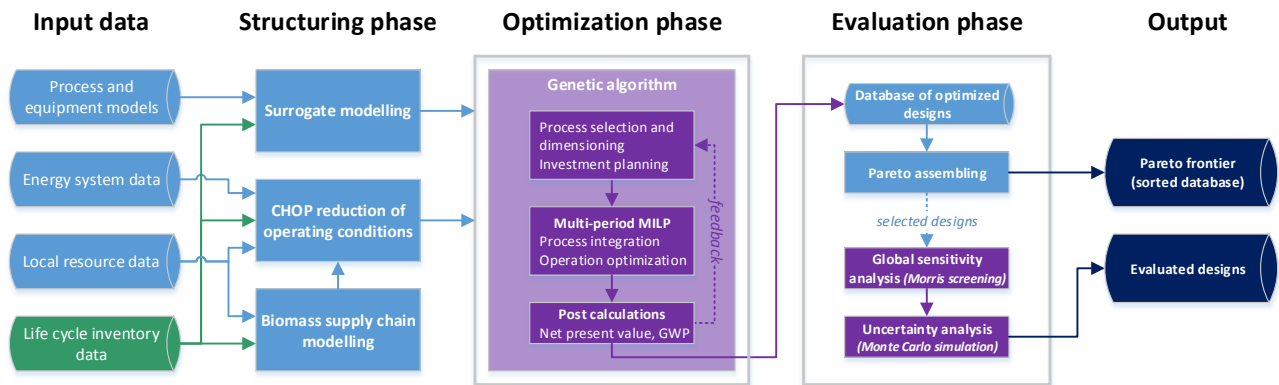
230 2.2. Methodology

231 As mentioned, a previously developed methodology for designing FMGs [6] was applied in this work. The
232 methodology structure is presented in Figure 5.

233 In short, the methodology applied is capable of conducting multi-objective design optimization of an FMG
234 superstructure whilst considering:

- 235 ○ Selection, location, and dimensioning of processes
- 236 ○ Systematic heat and mass integration using pinch analysis
- 237 ○ Flexible operation optimization with respect to both short-term market fluctuations and long-term
238 energy system development through the application of the Characteristic Operating Pattern (CHOP)
239 method [30]
- 240 ○ Investment planning
- 241 ○ Global sensitivity and uncertainty analysis
- 242 ○ Consideration of local resource availability, biomass supply chains, and market sizes
- 243 ○ Variable part-load performance

244 Input data to the design methodology includes process and equipment models, energy system data, local
245 resource data, and life cycle inventory data. The input data is structured prior to the optimization, which is
246 conducted by a hybrid genetic algorithm/mixed integer-linear programming model. The optimization
247 generates a database of designs with deterministic performances, for which Pareto analysis can be
248 conducted. A number of interesting designs may then be picked for further assessment, including
249 sensitivity and uncertainty analysis.



250

251

252

Figure 5: Design methodology structure [6]. The structure illustrates how input data is first structured, following which the primary optimization is conducted. The outcomes of the optimization are afterwards assessed further.

253

In the present case, the retrofit design was optimized with the aim of maximizing net present value (NPV) and minimizing the total CO₂ emission impact (TCE) from operating the system over the period 2015-2035. The TCE is a simple measure of the difference between CO₂ emissions from plant operation and replaced CO₂ emissions in the reference system. Investment planning and wood chips supply chains are not considered in the study.

254

255

256

257

258 2.3. Modelling and assumptions

259 2.3.1. Horsens CHP and district heating system

260

261

262

263

264

265

266

267

The two waste incineration boilers at Horsens CHP have a capacity of 5 tonnes of waste per hour each, and their minimum operation load is 75% [27][31]. Due to the demand for processing of local waste, the boilers were assumed to be operated at all times. The Rankine cycle was operated in back-pressure mode with a nominal power generation capacity of 7 MWe and a nominal heat generation capacity of 25 MJ/s [27]. The steam Rankine cycle has two condensers in order to optimize the overall exergy efficiency: One operated at 0.3 bar, and the other at 0.8 bar [27]. To comply with the district heating forward and return temperatures, it was assumed that 75% of the condensation heat was generated in the 0.8 bar condenser and that the generation of power and heat was directly proportional to the load.

268

269

270

Assuming that the exhaust gas from the gas turbine was used directly for district heating generation, with a nominal capacity 8 MJ/s [27], the nominal gas consumption and electricity generation capacities were calculated using estimated values of electrical efficiency and overall energy efficiency of the gas turbine.

271

272

273

The district heating system was assumed to have a maximum district heating demand equal to the heat generation potential of Horsens CHP. A forward/return temperature scheme of 90°C/40°C was assumed, and seasonal differences were neglected.

274

275

Operation data used in the modelling of Horsens CHP are presented in Table 1. Functions relating energy and mass flows in the system to operation variables are presented in Appendix A.

276

Table 1: Operation data used in the modelling of Horsens CHP.

Parameter	Notation	Value
RANKINE CYCLE		

waste incineration capacity	σ_{ran}	33.3 MJ/s [27] ^a
nominal power generation	P_{ran}	7.0 MWe [27]
nominal district heating generation	\dot{Q}_{ran}	25.0 MJ/s [27]
nominal heat in 0.8 bar condenser	$\dot{Q}_{ran,hp0}$	18.75 MJ/s
nominal heat in 0.3 bar condenser	$\dot{Q}_{ran,lp0}$	6.25 MJ/s
minimum load	$\lambda_{ran,min}$	0.75 [27][31]
variable operating costs	$c_{ran,var}$	15.9 €/MWh waste [31] ^b
energy efficiency	η_{ran}	0.96 [31]
GAS TURBINE		
nominal gas consumption	σ_{gt}	20.0 MWth
electrical efficiency	$\eta_{gt,E}$	0.4 [31]
energy efficiency	η_{gt}	0.8 [31]
off-gas temperature	$T_{gt,max}$	600°C
cooled exhaust gas temperature	$T_{gt,min}$	70°C
variable operating costs	$c_{gt,var}$	7.0 €/MWh gas [31]
minimum load	$\lambda_{gt,min}$	0.40 [31] ^c
DISTRICT HEATING SYSTEM		
maximum district heating demand	σ_{dh}	33.0 MJ/s
forward temperature	$T_{dh,fw}$	90°C
return temperature	$T_{dh,rt}$	40°C

277 ^a: Corresponding to a processing capacity of 10 ton/h of waste [31].

278 ^b: Corresponding to 53.0 Euro/ton of waste [31].

279 ^c: The minimum load is assumed constrained due to emission restrictions [31].

280 2.3.2. Butchery

281 Based on specialist knowledge collected by Energinet.dk, the shares of thermal utility demands in a typical
282 Danish butchery running on natural gas are presented in Table 2. The values were used to describe the
283 thermal utility demands of the butchery in the case study. It was assumed that the butchery had a nominal
284 energy utility demand of 6.43MWth³, that the thermal parts of the utility demand was met by a natural gas
285 boiler in the reference case, and that excess heat from thermal utility demands above 100°C could be
286 recovered and utilized directly for district heating generation. Operation data used in the modelling of the
287 butchery is summarized in Table 3. Functions for energy and mass flows in the system are presented in
288 Appendix A.

289 **Table 2: Average thermal utility demands in Danish butcheries.**

Thermal utility demand	Share of energy demand	Assumed temperature requirements
Boiling and evaporation	4%	110°C
Cleaning	37%	60°C
Process gas	35%	–
Room heating and losses	24%	35°C

290 **Table 3: Operation data used in the modelling of the butchery.**

Parameter	Notation	Value
Maximum thermal utility demand	σ_{ind}	6.43 MJ/s
Gas boiler operating costs	$c_{gb,var}$	0.5 €/MWh [31]

³ This capacity represents the capacity of an average butchery in Denmark, according to Energinet.dk.

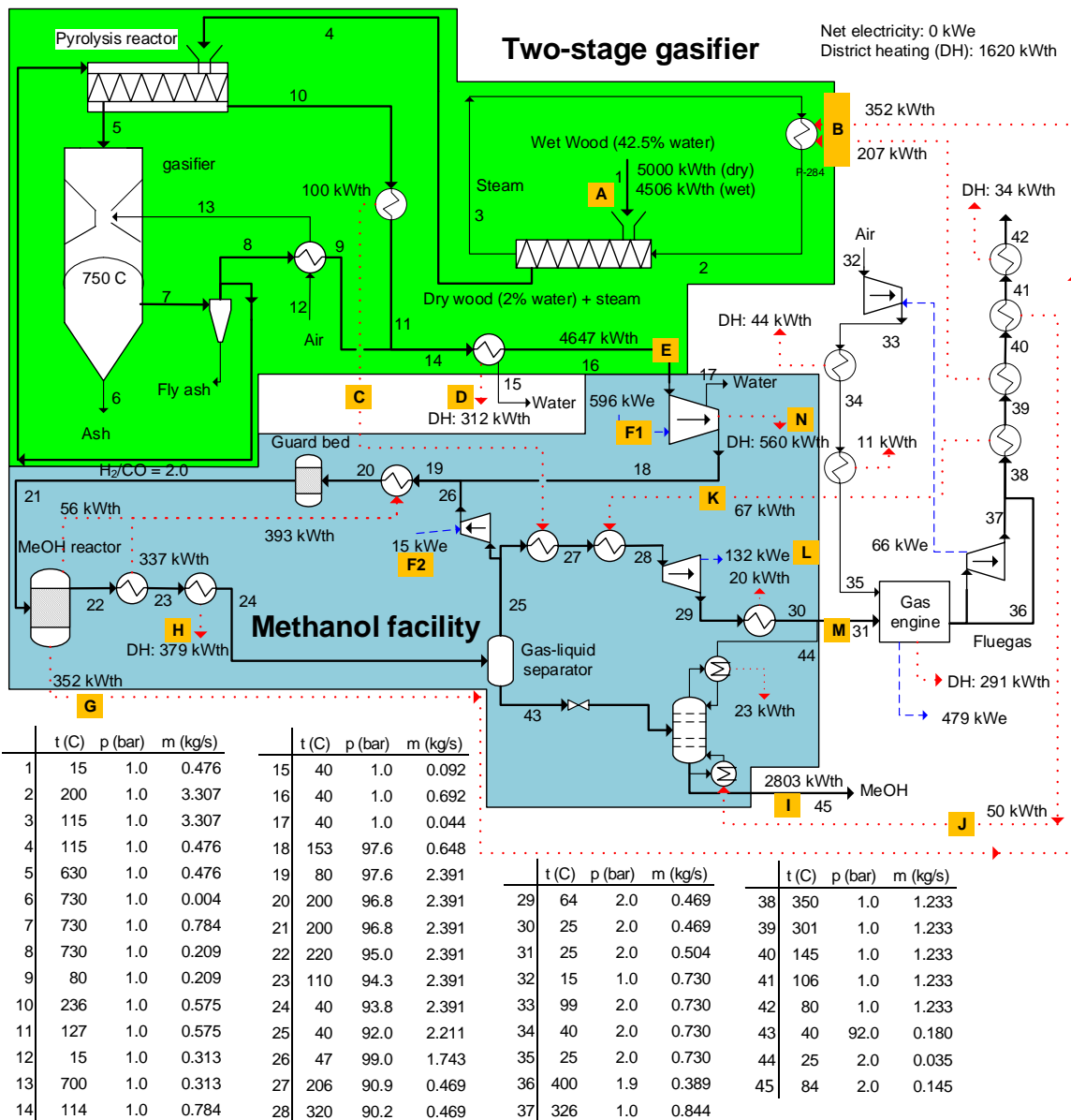
291 2.3.3. Biorefinery

292 The biorefinery considered was based on an upscaled version of the Two-stage Biomass Gasifier, a gasifier
293 concept which can generate a product gas almost free of tar (5 mg/Nm^3) and with a low methane content
294 [32]. The gasifier is air-blown and has been demonstrated in a size up to $1.5 \text{ MW}_{\text{th}}$ input [33]. The gas from
295 the gasifier is used by the biorefinery for methanol production and process heat generation, by the CHP for
296 heat generation, or by the butchery for process gas and heat. When the gasifier is air-blown, only a part of
297 the product gas can be converted to methanol because of nitrogen build-up in the methanol synthesis loop.
298 In order to increase the biomass to methanol conversion, an SOEC is included in the biorefinery. The SOEC
299 can supply pure oxygen for the gasifier and hydrogen for the methanol synthesis.

300 In the present work, a surrogate model of the biorefinery was developed based on the models presented
301 by Clausen et al. [28][29]. The gasifier was assumed fed by imported wood chips. The division of reference
302 components into surrogate models is illustrated in Figure 6. In addition to this, an SOEC model was
303 developed. Finally, a gas burner for burning un-reacted product gas was assumed installed on-site with the
304 biorefinery.

305 The integration of the SOEC increases the operational flexibility of the biorefinery, and the biorefinery can
306 generally be said to operate in one of the following three modes: 1) air-blown, 2) oxygen-blown, 3)
307 hydrogen boosted. In mode 2, the SOEC operates in part load, based on the oxygen demand of the gasifier.
308 In mode 3, the SOEC operates at full load based on the maximum feasible addition of hydrogen in the
309 methanol synthesis.

310 The energy conversion ratio of biomass-to-methanol for running in air-blown, oxygen-blown, and
311 hydrogen-boosted operation modes were identified from simulations of the reference model [28].
312 Assuming linear relations for SOEC loads between the three described operating modes, the biomass-to-
313 methanol energy ratio of the biorefinery as a function of SOEC load is plotted in Figure 7. The figure clearly
314 shows a bend in the curve at an SOEC load of 0.37, where the oxygen-blown operating mode is defined. The
315 slope of the curve to the left of the oxygen-blown point is about two times higher than the slope to the
316 right, meaning that the conversion of electricity to methanol, by means of an SOEC, is twice as efficient
317 below the full oxygen-blown operation point. The SOEC can therefore be allowed to operate in oxygen-
318 blown mode at a higher electricity price than what could be advantageous for the hydrogen-boosted mode.



319
320
321
322

Figure 6: Reference model of the wood chip-based two-stage gasifier and methanol facility, with surrogate model division outlined. Flows denoted with a letter are included in the surrogate model, see Appendix A. Modified version of a figure from Clausen [28].

323
324
325
326
327
328

In hydrogen-blended mode almost all the carbon in the product gas could theoretically be converted to methanol, but in the present biorefinery design the carbon-to-methanol conversion is constrained to 89%⁴. In oxygen-blown mode 66% of the carbon in the product gas is converted to methanol (practically all CO is converted), while in air-blown mode 41% of the carbon is converted to methanol. Only in air-blown mode will the unreacted product gas contain significant amounts of energy and therefore allow for export of this mass flow to the butchery.

⁴ The carbon conversion could be increased to 97% by recirculating the CO₂ from the topping column (stream 44 on Figure 6) to the methanol synthesis loop.

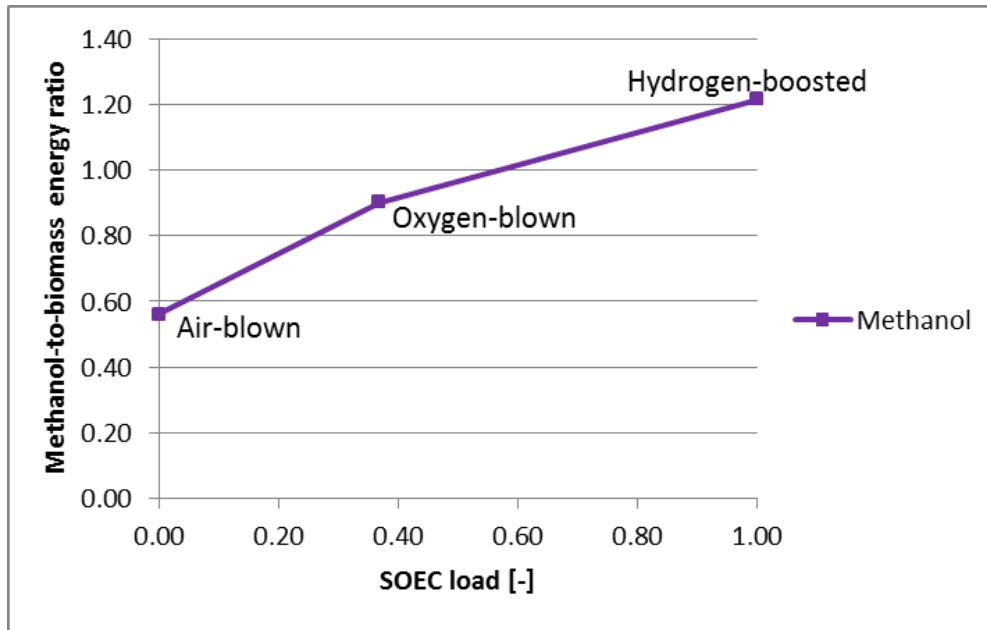


Figure 7: Methanol-to-biomass energy conversion ratio for different SOEC loads.

329
330

331 Operation data used in the biorefinery model is summarized in Table 4, while functions for energy and mass
332 flows in the system are included in Appendix A. It was assumed that operation and maintenance costs for
333 the biorefinery, excluding resource consumption costs, were independent of operation. Sales of excess
334 oxygen were not considered.

335

Table 4: Operation data used in the biorefinery model.

Parameter	Notation	Value
Biomass-to-product gas efficiency	$\eta_{gasifier,NCV}$	0.93 [28]
SOEC power-to-hydrogen efficiency	$\eta_{SOEC,NCV}$	0.92 ^a
Reference dimension	$\sigma_{0,bio}$	360 MJ/s wood chips [34]
Reference investment cost	$C_{inv,bio0}$	314.9 M€ [31][34] ^b
Reference fixed annual operating costs	$C_{op,bio}$	9.2 M€/year [31][34] ^b

336 ^a Efficiency calculated by assuming an inlet temperature of 770 °C and an outlet temperature of 800 °C combined with the
337 assumption that 5% of the electricity is lost (heat losses, inverter loss, and electricity consumption by blowers etc.) [35].

338 ^b: Investment and fixed operating costs are calculated for the combined biorefinery, with an SOEC dimensioned for maximum
339 hydrogen boost of the methanol production.

340 2.3.4. Infrastructure and industrial heat pumps

341 In the case study, investments in district heating and gas infrastructure for connecting the two areas were
342 considered. The distance between the areas was set to be 9km. Costs of infrastructure investments used in
343 the case study are summarized in Table 5. Infrastructure operation and maintenance costs were neglected.

344 The forward district heating water could be utilized as heat source for ammonia-water hybrid heat pumps
345 that may provide process heating at temperatures of up to 140°C [36]. In the case study, it was assessed if
346 such heat pumps would be beneficial for meeting the boiling and evaporation thermal utility demands of
347 the butchery. A scalable surrogate model of an ammonia-water hybrid heat pump was developed based on
348 a reference model presented by Jensen et al. [36]. Data used in the modelling of the heat pump are
349 presented in Table 6, while functions for thermal and mass flows are summarized in Appendix A.

350

Table 5: Infrastructure investment costs.

Parameter	Notation	Specific costs	Investment cost
District heating connection of butchery	$C_{inv,DH}$	195 €/m ^a	1.76 M€
Gas pipe between Horsens CHP and butchery	$C_{inv, gas}$	130 €/m ^b	1.17 M€

351

^a: Assuming that a district heating pipe with inner/outer diameter of 0.89m/2.80m is trenched beneath asphalt roads [37].

352

^b: Assuming investment costs equivalent to hydrogen pipes with an inner diameter of 160 mm and a flow pressure of 1 to 4 bars.

353

This size is considered adequate for a peak supply of approximately 14 MJ/s syngas. Operation and maintenance costs are neglected [38].

354

355

Table 6: Data used in the ammonia-water hybrid heat pump model.

Parameter	Notation	Value
Source inlet temperature	T_{source}	90°C
Source temperature difference	ΔT_{source}	50°C
Sink inlet temperature	T_{sink}	120°C
Sink temperature difference	ΔT_{sink}	10K
Temperature lift	ΔT_{lift}	50°C ^a
Coefficient of performance	COP	2.9 [36] ^b
Reference investment cost	$C_{inv, hp0}$	0.43 M€ ^b
Reference heat pump dimension	σ_{hp0}	1.0 MJ/s sink heat ^b
Operating cost	$C_{op, hp}$	4900 €/(MJ/s – year) [31] ^c

356

^a: The temperature lift is set as the difference between average DH temperature and sink outlet temperature.

357

^b: The values are taken for an ammonia-water hybrid heat pump with sink and source temperature lifts of 10K and with optimized ammonia fraction and circulation ratio for the given operating scheme, as predicted by Jensen et al. [36].

358

359

^c: The heat pump operating costs are assumed equal to the highest predicted operating costs of an electric district heating heat pump [31].

360

361

2.4. Energy system data

362

Three reference years were used for describing the energy system development over the period 2015-2035,

363

namely 2015, 2025, and 2035. The energy system data for 2015 was assumed repeated for the first six

364

years, the data from 2025 was assumed repeated for the following eight years, while the data for 2035 was

365

assumed repeated for the final six years of the period.

366

Table 7: Fuel prices in the reference years.

Parameter	2015 scenario	2025 scenario	2035 scenario	Reference
Natural gas	9.66 [€/GJ]	9.93 [€/GJ]	10.51 [€/GJ]	[39]
Wood chips	6.52 [€/GJ]	6.90 [€/GJ]	7.52 [€/GJ]	[39]
Methanol	21.25 [€/GJ] ^a	24.63 [€/GJ] ^a	28.34 [€/GJ] ^a	[39]
Gasoline	20.73 [€/GJ]	23.68 [€/GJ]	25.42 [€/GJ]	[39]
CO ₂ quota, intermediate estimate	7.41 [€/ton]	13.62 [€/ton]	42.21 [€/ton]	[39]
Oil ^b	13.72 [€/GJ]	16.51 [€/GJ]	18.16 [€/GJ]	[39]

367

^a: The methanol price is calculated as the estimated gasoline value plus the estimated economic value of avoided CO₂ emissions with respect to CO₂ quota value.

368

369

^b: To be consistent with data, the fuel oil price corresponds to the predicted oil price from [39] and not the actual oil price, which by March 2016 is around 40 USD/barrel, corresponding 6.11 [€/GJ] [40].

370

371

As illustrated in Figure 3 and Figure 4, the FMG interacts with the surroundings through the import and/or

372

export of power, natural gas, district heating, waste, wood chips, and methanol. Waste is assumed to be

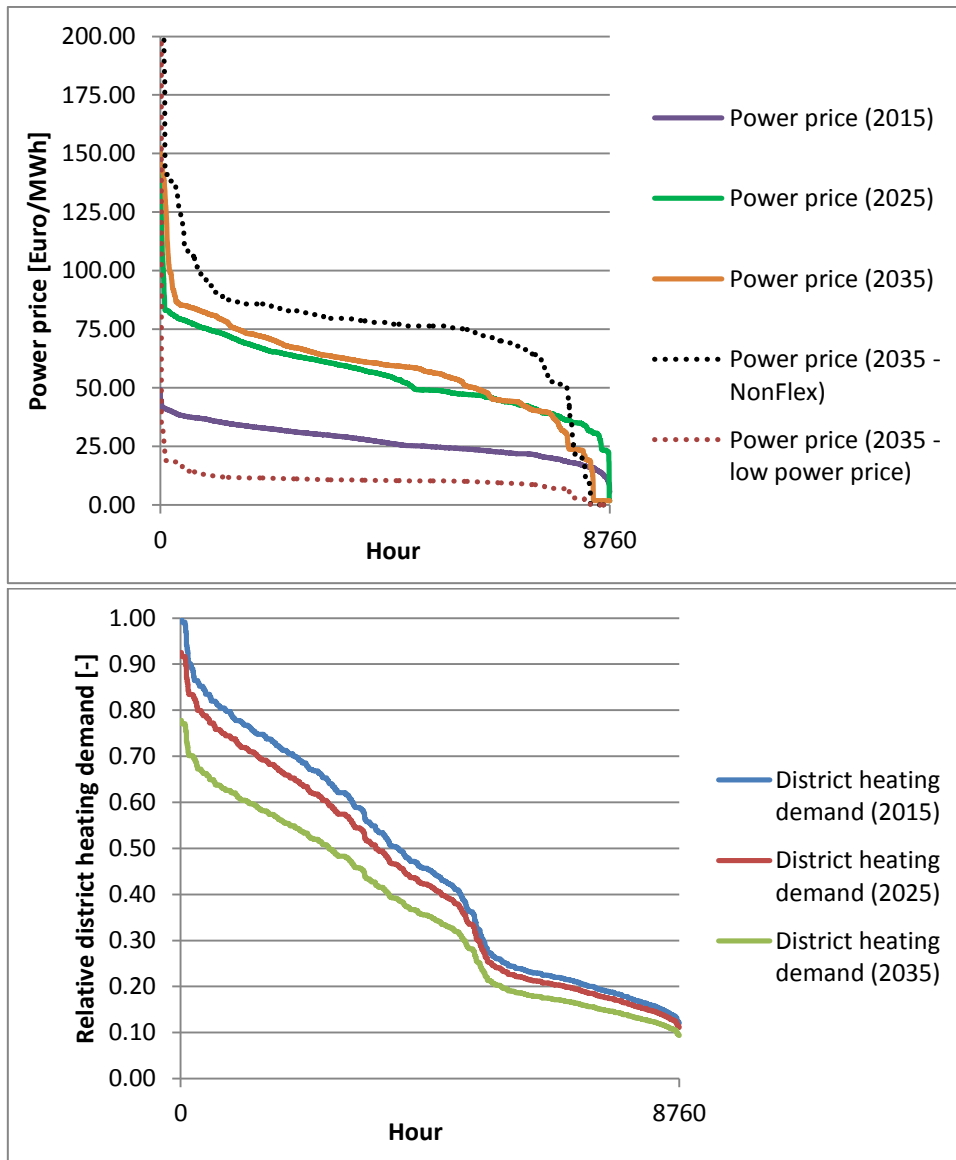
373

free as the FMG is obliged to provide waste processing. Prices for natural gas, wood chips and methanol in

374

each of the three reference years are presented in Table 7.

375 The FMG was considered to be the sole provider of district heating and industry energy utility, so the
 376 district heating demand and industry energy utility demand had to be met by the FMG at all times.

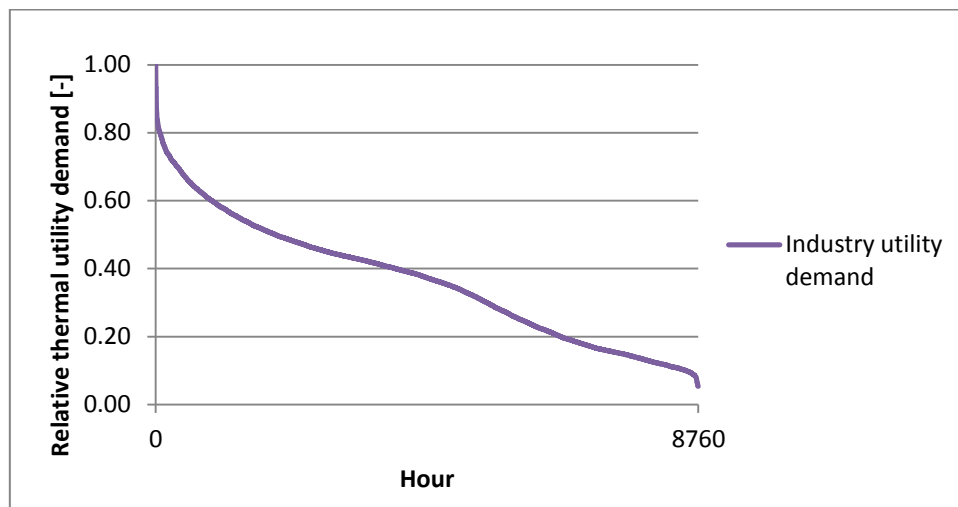


377
 378
 379 **Figure 8: Annual duration curves for the power price and relative district heating demand in Horsens in each of the three**
 380 **scenarios.**

381 For the reference scenario, the district heating demand and expected power price were extracted from
 382 simulations within the energy system model SIFRE [41]. SIFRE is an energy systems modelling tool
 383 developed to handle flexible, integrated energy systems and include accurate representation of new
 384 components such as renewable energy production, flexible demand, and new types of energy carriers as
 385 for instance various green gasses. SIFRE simulates each power plant individually and solves the unit
 386 commitment problem for an optimal production schedule. SIFRE simulates the existing day-ahead market
 387 and generates electricity prices which are used as boundary conditions, assuming that the operation of the
 388 FMG is not affecting the national prices considerably. The three scenario simulations for 2015, 2025 and
 389 2035 were based on Energinet.dk's analysis assumptions [42]. Duration curves for the power price and
 390 district heating demand for each of the scenarios are presented in Figure 8. In addition, two other duration

391 curves for 2035 are included in the figure: one from the NonFlex scenario, in which power prices were
392 extracted from a different energy system simulation scenario based on the assumption that smart grid
393 technology will not obtain a major breakthrough in Denmark, meaning that the operation of electric
394 vehicles, individual heat pumps and electrolysis plants is not optimized for the electricity price [43]. And a
395 low power price scenario, in which power prices in 2035 has been reduced by a factor 7.5 as compared to
396 the NonFlex scenario, to assess what impact extremely low and highly variable power prices would have on
397 the system performance.

398 Data on annual butchery thermal utility demand was assumed similar for each year of the period. The
399 demand profile was provided by Energinet.dk and is based on the hourly natural gas consumption of a
400 number of Danish food industries in 2014. The duration curve is presented in Figure 9.



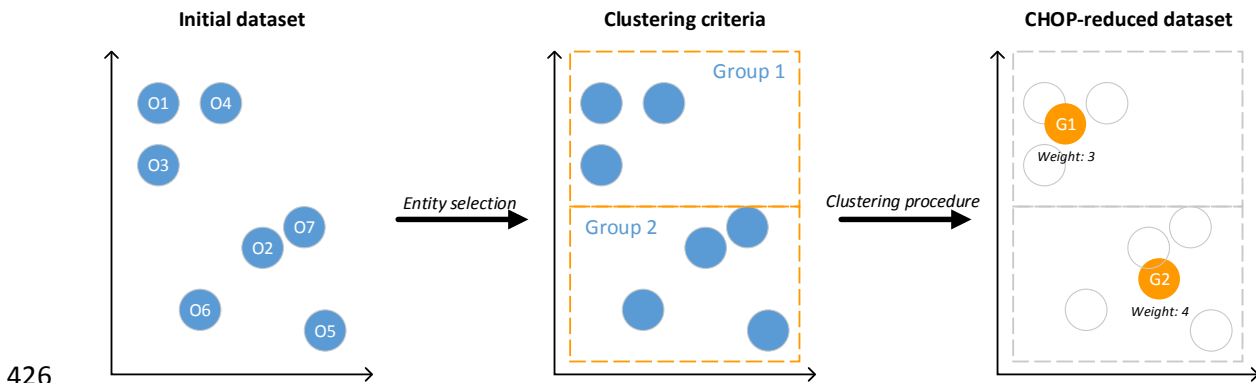
401
402 **Figure 9: Relative industry thermal utility demand duration curve for one year.**

403 As the system can be looked upon as replacing an existing district heating supply system and a reference
404 industrial energy supply system, neither CO₂ emission replacements nor incomes are associated with
405 district heating and industry thermal utility generation. Instead, the resulting NPV and TCE of the FMG may
406 be compared with those of the reference system to assess the performance of the retrofitted system.

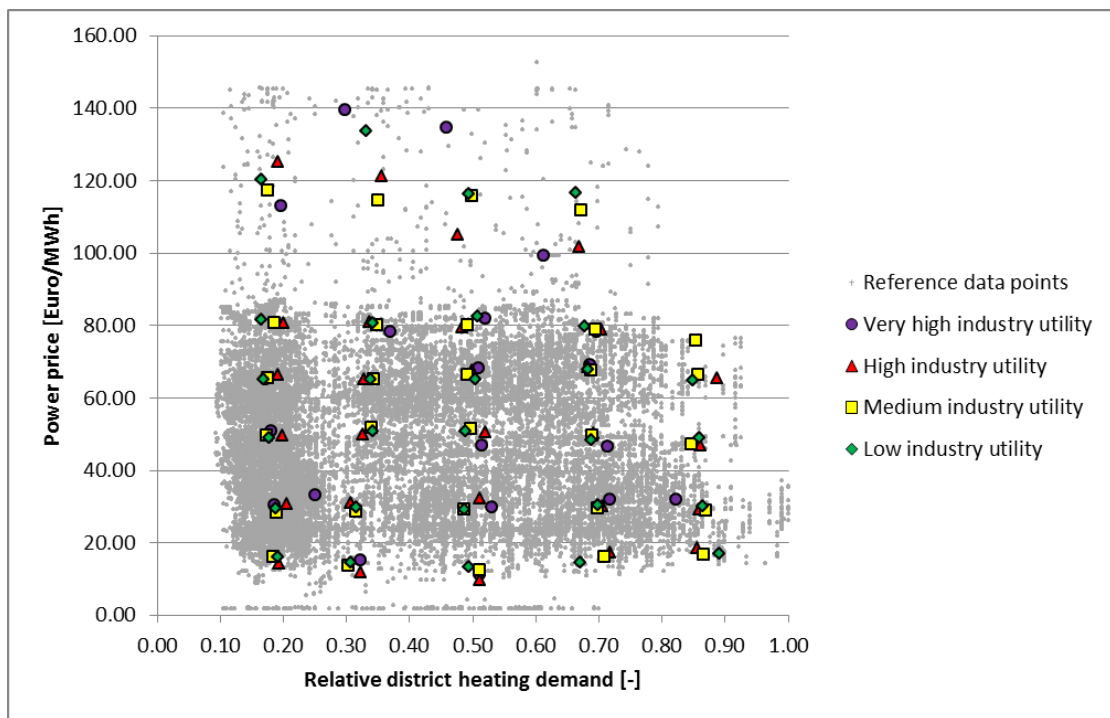
407 Four additional scenarios were considered for assessing performance uncertainties of selected designs: A
408 low fuel price scenario, in which the methanol selling price was reduced by 25% compared to the reference
409 scenario; a high fuel price scenario, in which the methanol selling price was increased by 25% compared to
410 the reference scenario; a NonFlex power scenario, in which power prices for 2035 were taken from the
411 NonFlex scenario as described previously [43]. And a low power price scenario, in which power prices in
412 2035 has been reduced by a factor 7.5 as compared to the NonFlex scenario.

413 Regarding TCE calculations, average emissions from power generation in the Danish energy system were
414 used to represent the emissions of consumed or generated electricity. For 2015, the average CO₂ emission
415 from power generation was set to 270 kg/MWh, while it was set to 112 kg/MWh for 2025 and 2035 [42].
416 The CO₂ emission associated with waste combustion was set to 37.0 kg/GJ [44]. A CO₂ emission of 57.0
417 kg/GJ was associated with natural gas combustion, while methanol was assumed to replace gasoline with
418 an energy ratio of 1:1 and thereby resulting in a CO₂ emission reduction of 73.0 kg/GJ [42]. The wood chips
419 were assumed to be CO₂ neutral in the study.

420 In order to reduce computation time of the operation optimization, the external operating condition
 421 dataset was reduced using the Characteristic Operating Pattern (CHOP) method for data aggregation [30].
 422 In short, the CHOP method is a visually-based aggregation method which clusters operating points with
 423 similar parameter values in representative data points called CHOP groups. The operation optimization is
 424 then conducted for the CHOP groups rather than for each operating point, significantly reducing the
 425 computational effort. The clustering principle is illustrated in Figure 10.



426
 427 **Figure 10: Principal sketch of the data aggregation principle applied in the CHOP method [30]. Operating points O_j are clustered**
 428 **and merged into CHOP groups G_j with aggregated weight factors.**



429
 430 **Figure 11: Scatter plot of the reference dataset and the aggregated dataset with respect to relative heating demand and power price.**
 431 **Note that the third dimension, industry utility demand, is not visible for the reference data points and that the duration**
 432 **(weight) of the aggregated points depends on the amount of reference points in their vicinity. For more information, refer to**
 433 **Appendix B.**

434 In the present case, five volatile external operating conditions were identified using the CHOP approach:
 435 Power price, district heating demand, butchery thermal utility demand, wood chips price, and methanol
 436 price. Natural gas was not considered as a volatile external operating condition as the absolute variation

437 within the scenario was less than 10%. In order to minimize the number of CHOP groups to consider, data
 438 clustering was only conducted with respect to power price, district heating demand, and butchery thermal
 439 utility demand as they were the parameters with the largest volatility. The accuracy error of not clustering
 440 for methanol, natural gas, and wood chip prices was assessed a posteriori. The entire CHOP method
 441 procedure is described in Appendix B, and the resulting CHOP datasets are presented for all scenarios as
 442 well. Reference operating points and resulting CHOP groups of the reference scenario are illustrated in
 443 Figure 11.

444 2.5. Optimization model

445 The system was optimized with respect to maximizing NPV and minimizing TCE over the period 2015-2035.
 446 Design variables for the optimization model are summarized in **Error! Reference source not found.**, while
 447 operation variables are summarized in Table 9.

448 **Table 8: Design variables in the case study optimization problem.**

Design variable	Notation	Type	Lower bound	Upper bound
Biorefinery dimension [MWth biomass]	σ_{bio}	Continuous	5.0 MWth	200.0 MWth ^a
Biorefinery location	ω_{bio}		Integer	
Product gas connection between areas	ω_{gas}		Integer	
District heating integration at butchery	ω_{DH}		Integer	

449 ^a: The upper bound of 200 MWth corresponds to a medium-sized methanol-producing biorefinery based on the selected
 450 technology [34], and it is estimated that larger facilities cannot be accommodated on the site due to infrastructure constraints.

451 **Table 9: Operation variables in the case study optimization problem.**

Horsens CHP operation variables	Notation	Type	Lower bound	Upper bound
Rankine cycle load	λ_{ran}	Continuous	0.75[31]	1.00
Gas turbine load	λ_{gt}	Continuous	0.40 ^a	1.00
SOEC load	λ_{SOEC}	Continuous	0.00	1.00
Methanol production load	λ_{MeOH}	Continuous	0.00	1.00
Gas boiler load	$\lambda_{gb,ind}$	Continuous	0.00	1.00
Industrial heat pump load	$\lambda_{hp,ind}$	Continuous	0.00	1.00

452 ^a: Minimum load constrained due to exhaust emission constraints [31].

453 The NPV, C_0 , was calculated as a function of investments costs $C_{inv,k}$ and hourly operation result $c_{op,i}$ times
 454 the present value time factor $t_{PV,i}$ for each period i . The facility to be installed was given a lifetime of 20
 455 years, and an interest rate of $r = 0.05$ was applied in net present value calculations.

$$456 C_0 = -\sum_k C_{inv,k}(\sigma_k, \omega_k) - \sum_i c_{op,i}(\lambda_i) \cdot t_{PV,i} \quad (1)$$

457 Investment costs for each facility was calculated as

$$458 C_{inv,k}(\sigma_k, \omega_k) = \omega_k C_{inv,k0} \left(\frac{\sigma_k}{\sigma_{k0}} \right)^{p_f} \quad (2)$$

459 Here, $C_{inv,k0}$ is the reference investment cost and σ_{k0} is the reference dimension of the facility. A power
 460 factor of $p_f = 0.75$ was used for economy-of-scale calculations.

461 The present value time factor for each reference data point was calculated as

462 $t_{PV,i} = t_i \frac{1}{(1+r)^T}$ (3)

463 Here, T is the number of years from the installation of the FMG, and t_i is the duration of the period.

464 The TCE, Z_0 , was calculated as the sum of hourly emission results $z_{op,i}$ for each period i times the duration
465 of the period t_i .

466 $Z_0 = \sum_i z_{op,i}(\lambda_i) \cdot t_i$ (4)

467 The hourly emission result $z_{op,i}$ is calculated as the sum of emissions related to FMG operation minus the
468 sum of emissions from replaced production.

469 $z_{op,i}(\lambda_i) = \sum_i z_{emitted,i}(\lambda_i) - \sum_i z_{replaced,i}(\lambda_i)$ (5)

470 Process integration was conducted for both areas. A pinch temperature of 10K was used for integration of
471 thermal streams, apart from in the condensers of the steam Rankine cycle where a pinch temperature of
472 3.5K was used. The investment cost of the heat exchanger network was estimated for each assessed design
473 as a part of the pinch analysis using a method from Turton et al. [45]. Further information can be found in
474 Bolliger [46].

475 The optimization model to be solved in the case study can be written in condensed form as

476
$$\begin{cases} \min_{\omega_k, \sigma_k, \lambda_{k,i}} \begin{cases} -C_0 \\ Z_0 \end{cases} \\ \text{with variables} \\ \omega_k \in \{0,1\} \\ \sigma_k \in [\sigma_{k,min}, \sigma_{k,max}] \\ \lambda_{k,i} \in [\lambda_{k,min}, \lambda_{k,max}] \end{cases} \quad (6)$$

477 The problem (6) was solved using the hybrid genetic algorithm/mixed integer-linear programming approach
478 as described in Lythcke-Jørgensen et al. [6]. The genetic algorithm was run for 6 generations with a
479 population size of 20.

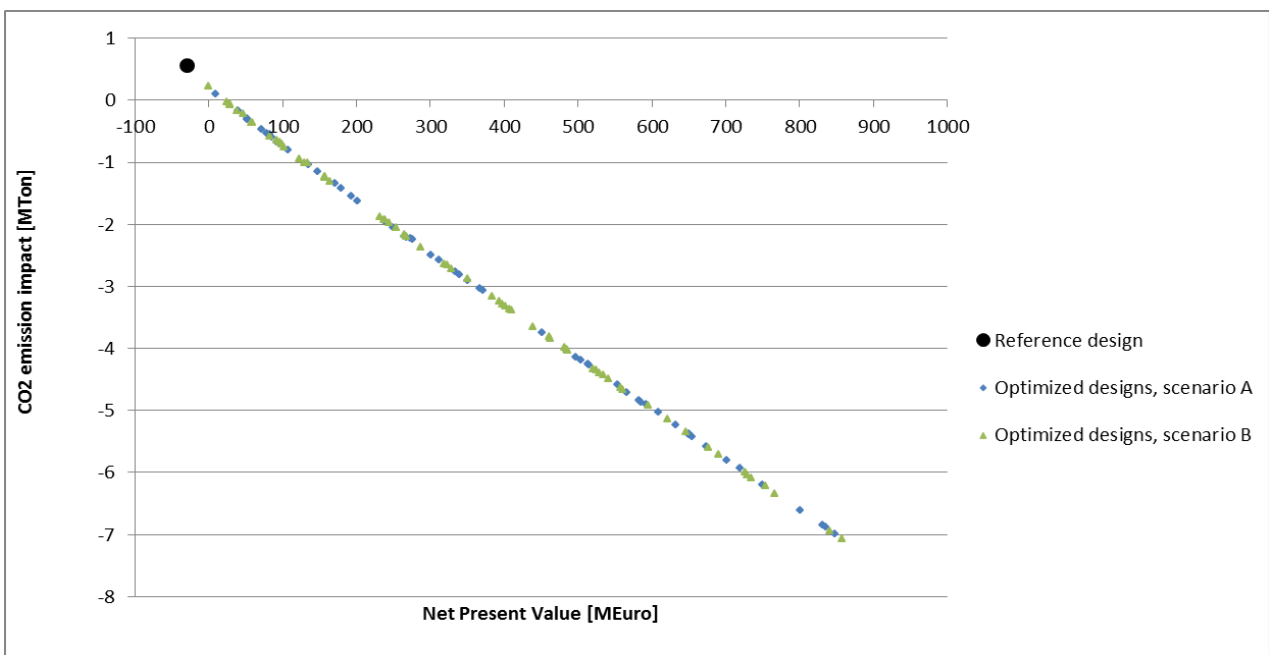
480 3. Results

481 3.1 Design optimization

482 Running the optimization procedure for (6), a database of optimized design solutions was obtained. Figure
483 12 presents a scatter plot illustrating the performances of optimized solutions with respect to NPV and TCE.

484 First of all, the figure illustrates that under the set conditions and assumptions, there is no trade-off
485 between reducing TCE and maximizing NPV for the FMG designs. This outcome suggests that the
486 biorefinery is competitive for the price schemes considered, and that the upper bound on NPV is defined by
487 the constraint on the biorefinery dimension for the given site. It must be emphasized that taxes, subsidies
488 and similar aspects were not considered in the economic calculations.

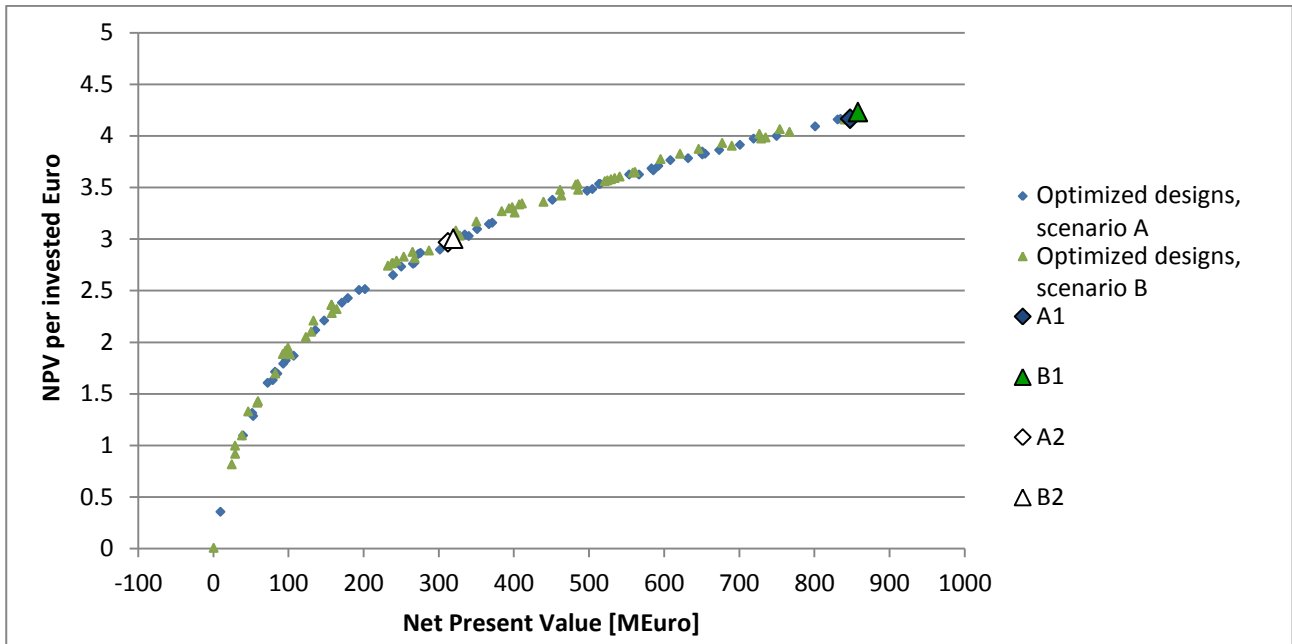
489 Regarding environmental impact, it was found that the larger the biorefinery dimension, the lower the TCE.
490 In addition, most of the proposed designs obtain a negative TCE, suggesting that energy generation in these
491 designs would replace generation with higher specific CO₂ emission levels in the reference energy system.
492 Secondly, it was found that designs having the biorefinery located next to the local industry (Scenario B)
493 performed better with respect to both objectives than designs where the biorefinery was located next to
494 the CHP unit (retrofit scenario A). This was primarily due to integration synergies, as a part of the reference
495 natural gas consumption of the butchery could be replaced by process heat and unreacted product gas
496 from the biorefinery. In Scenario A, the same replacement of natural gas consumption in the butchery
497 required investments in district heating and gas infrastructure and industrial heat pumps. However, the
498 overall synergy benefits only resulted in a few percent increase NPV and similar reduction in TCE for similar
499 biorefinery dimensions, meaning that impacts from synergies were only marginal compared to the overall
500 impact of installing a large-scale biorefinery.



501

502

Figure 12: Scatter plot of optimized design solutions with respect to NPV and TCE.



503

504

Figure 13: Scatter plot of optimized design solutions with respect to NPV and TCE.

505 In addition, the end results are found to have an almost linear profile, suggesting that nonlinear impacts
 506 from economy-of-scale in investments have little impact on the overall results when compared to linear
 507 operation impacts. The importance of various input parameters and associated performance uncertainties
 508 are assessed in the next section. However, it must be stressed that in the present study, district heating and
 509 industry utility services were included as constraints that had to be met, and economic benefits of meeting
 510 them were neglected. In case fixed costs were considered for these services, it would have a fixed positive
 511 impact on all NPVs. In addition, if costs were considered for cooling excess process heat were considered,
 512 this would have a negative impact for designs with larger biorefinery dimensions. Together, these effects
 513 would perhaps improve the significance of process integration benefits in the case study, which may in fact
 514 lead to a trade-off between economy-of-scale and process integration benefits.

515 Investigating the benefits of investments, a plot illustrating the relation between NPV and NPV per invested
 516 Euro is presented in Figure 14. The plot illustrates how the relative payback on investments increases with
 517 increasing NPV, and thereby biorefinery dimension. It is also found that relative investment payback in
 518 general is a few percent higher for retrofit scenario B than for retrofit scenario A.

519 3.2 Uncertainty analysis

520 Four optimized designs were selected for uncertainty analysis: The two retrofit designs with the highest
 521 NPV for both retrofit scenarios (A1 and B1), and two optimized designs with a biorefinery dimension of
 522 approximately 80.0 MWth (A2 and B2), representing medium-scaled design solutions. Design and
 523 performance characteristics of the selected designs are summarized in Table 10.

524

Table 10: Design and performance characteristics of the four selected FMG designs.

Design solution	NPV [M€]	CO ₂ emission impact [MTon]	σ_{bio}	ω_{DH}	ω_{gas}
A1	847.3	-6.98	199.3	0	1
A2	312.0	-2.57	81.2	1	0

B1	857.6	-7.07	199.9	0	0
B2	319.0	-2.63	82.4	1	0

525

Table 11: Input parameter uncertainties considered in the investment cost uncertainty analysis.

Parameter	Notation	Minimum value	Maximum value	Distribution
Biorefinery reference investment cost	$C_{inv,bio0}$	236.18 M€	393.63 M€	Uniform
District heating connection, investment cost	$C_{inv,DH}$	1.31 M€	2.19 M€	Uniform
Gas infrastructure, investment cost	$C_{inv,gas}$	0.88 M€	1.46 M€	Uniform
Heat pump reference investment cost	$C_{inv,hp0}$	0.32 M€	0.54 M€	Uniform
Power factor	p_f	0.6	0.9	Uniform

526

Variations in estimated NPV from uncertainties in investment costs and economy-of-scale benefits were assessed by applying the Monte Carlo simulation procedure presented by Sin et al. [47]. Reference investment costs were given a uniform uncertainty in the interval of $\pm 25\%$, while the power factor p_f was given a uniform uncertainty in the interval $\pm 20\%$. An overview of the uncertainties associated with various input parameters is given in Table 11.

527

528

529

530

531

For each Monte Carlo simulation, a sample of 1000 data points was generated using Latin Hypercube Sampling [48] and assuming zero correlation between uncertainties in input parameters. Running Monte Carlo simulations for all selected designs, the resulting 10th to 90th percentile intervals of predicted NPV for the designs are shown in Figure 14.

532

533

534

535

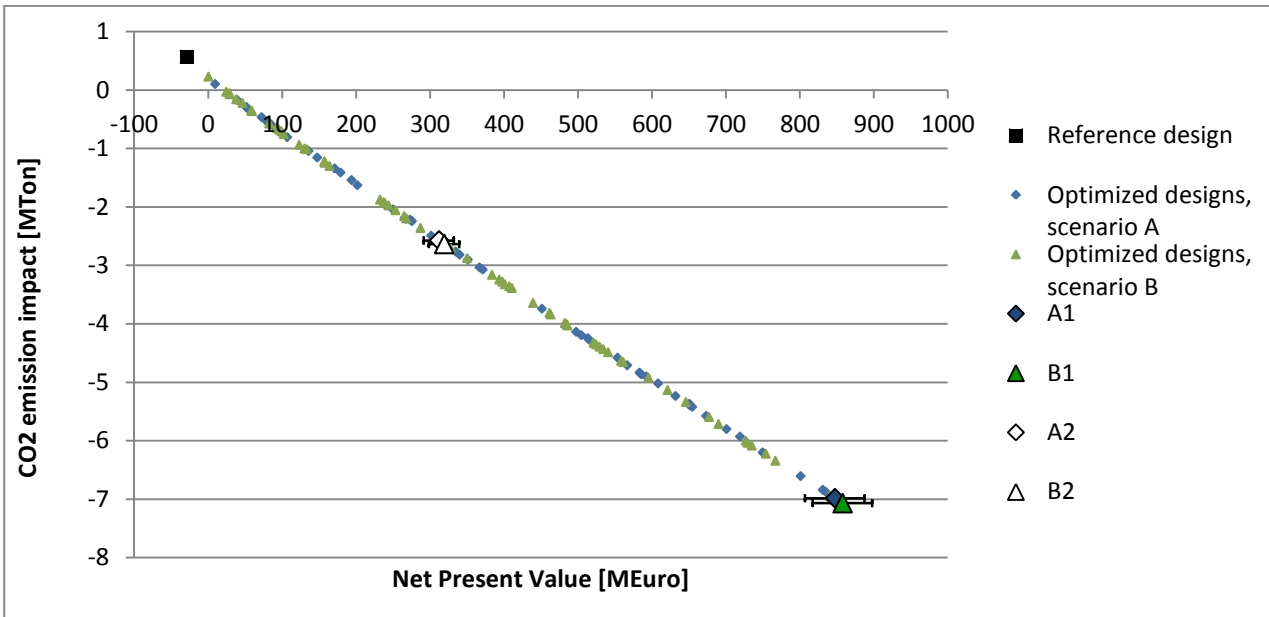
The results suggest that the considered uncertainties for investment costs would lead to NPV variations of $\pm 7\%$. Absolute variations in NPV were larger for designs A1 and B1, which was expected as absolute investment costs were higher for these designs. The outcomes illustrate that the investment uncertainties considered are not likely to have a significant influence on the overall performance of the designed FMGs over the 20 year period.

536

537

538

539

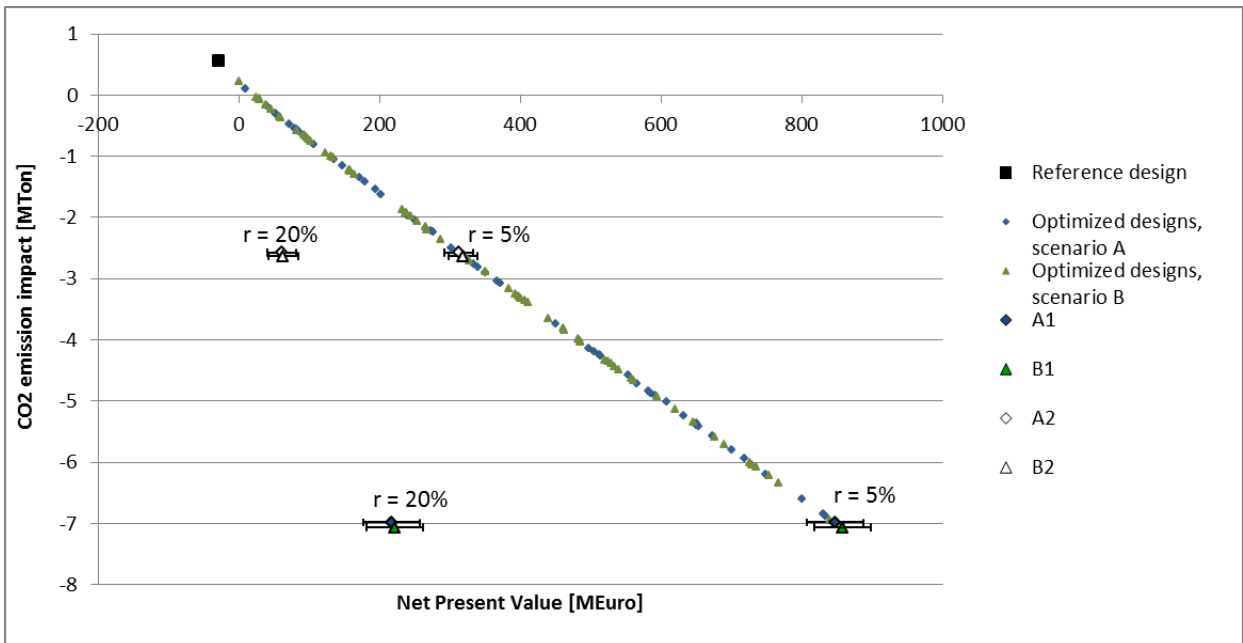


540
541
542

Figure 14: Selected designs and associated 10th to 90th percentile NPV performance variability in response to the investment cost uncertainties described in Table 11.

543
544
545
546
547

In addition to the uncertainty related to investment costs, the impact of changes in the interest rate applied in the NPV calculations was assessed. For each of the four selected designs, the operation optimization was conducted using an interest rate of 20% instead of the 5% to represent a high interest rate which could be expected in a private economic business case. The results, including 10th to 90th percentile intervals of predicted NPV based on investment cost uncertainties, are shown in Figure 15.



548
549
550

Figure 15: Performance of the four selected designs, including uncertainties related to investment costs, when changing the applied interest rate from 5% to 20%

551
552

The NPV was found to be reduced by 74%-80% for the four selected designs when the interest rate was increased to 20%, which was expected as an interest rate of 20% would make it much less attractive to

553 invest in the project when compared to a situation with an interest rate of 5%. Uncertainties related to the
554 applied interest rate are therefore likely to have a markedly higher impact on the NPV than the assumed
555 uncertainties related to investment costs.

556 Another interesting outcome is the finding that the uncertainties related to investment costs will have a
557 relatively larger impact on the NPV uncertainty for larger interest rates. This is because investment costs
558 are unaffected by the interest rate in NPV calculations, meaning that the absolute impact is constant while
559 the overall NPV is reduced for larger interest rates. Hence, the larger the interest rate, the larger the
560 relative impact of uncertainties in investment costs.

561 In order to assess the impact of uncertain operating conditions, the performances of the four selected
562 designs were assessed for each of the four additional energy system scenarios defined in Section 2.4: A high
563 fuel price scenario, a low fuel price scenario, the NonFlex scenario, and a low power price scenario. The
564 outcomes are illustrated in Figure 16.

565 From the figure, it is evident that methanol price uncertainties considered had a much higher influence on
566 NPV than uncertainties in investment costs. An increase of 25% in methanol price in the high fuel price
567 scenario increased the NPVs of the four selected designs by 67%-75%, while a similar reduction in methanol
568 price of 25% in the low fuel price scenario resulted in NPV reductions of 66%-74%. Also the low power price
569 scenario was found to have a larger impact on NPV variations than the considered uncertainties in
570 investment costs. Opposed to this, changes in NPV from the NonFlex scenario were comparable with
571 expected variations from investment cost uncertainties.

572 In addition, the TCE was found to increase in the low fuel price and NonFlex scenarios for all designs, owing
573 to the fact that the power-to-methanol price ratio was increased, making SOEC operation uncompetitive in
574 some periods. In consequence, hydrogen-boosted SOEC operation was terminated approximately 21% of
575 the time in the low fuel price scenario, while it was terminated for a bit more than 4% of the time in the
576 NonFlex scenario. Opposed to this, the TCE was only marginally affected in the high fuel price and low
577 power price scenarios as the SOEC was already operated in hydrogen-boosted mode for more than 98% of
578 the time in the reference scenario, meaning that the potential of increasing methanol production was very
579 limited.

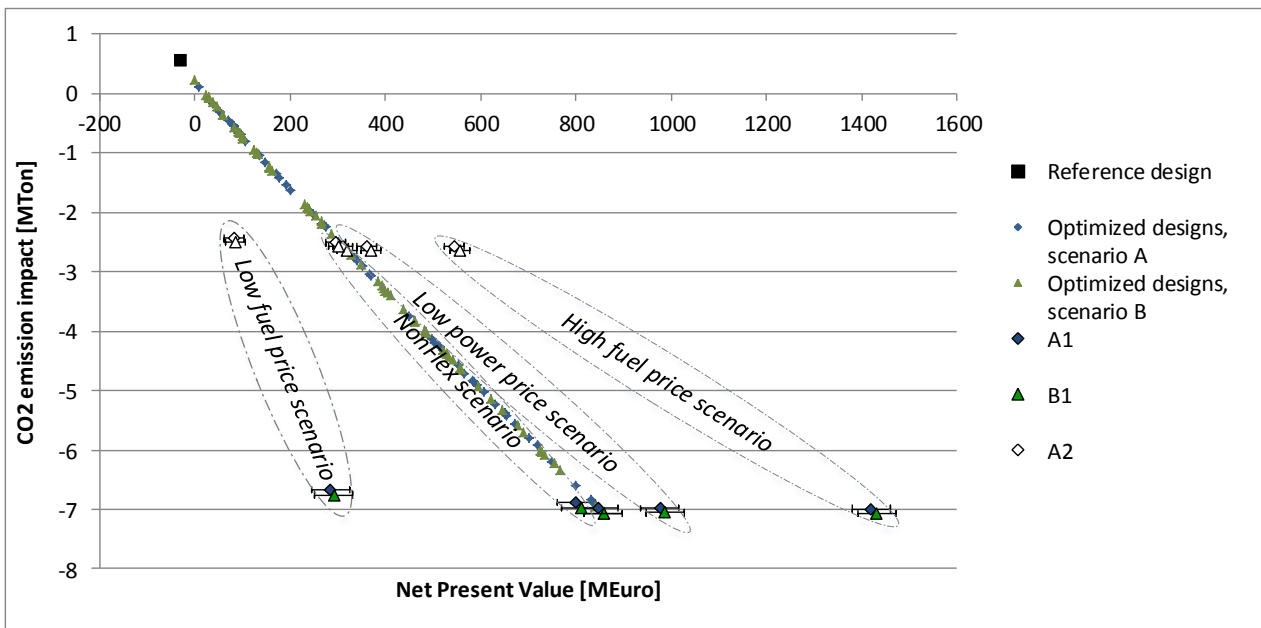


Figure 16: Performance of the four selected designs under various energy system scenarios. Results of the investment cost uncertainty analysis are indicated as well.

580
581
582

583 For the NonFlex scenario, the NPV was slightly reduced for all designs. This was caused by the higher power
584 prices over the last six years for this scenario, which increased the costs of SOEC operation and thereby
585 reduced the income from methanol sales.

586 To summarize, changes of $\pm 25\%$ in the methanol price were found to have a major impact on the
587 estimated performances of the FMGs in the case treated. The NPV of the optimal design solution, design B1,
588 was estimated to vary within the range 252.5 M€ to 1471.6 M€ in response to the assessed input
589 uncertainties on investment costs and operating conditions. Changing the interest to 20%, the lowest
590 estimated NPV of the design in the reference scenario was as low as 181.3 M€. For the optimal medium-
591 sized design, design B2, the relative NPV variation was found to be even larger. In general, the outcomes
592 stress the importance of including uncertainty analysis when designing and optimizing FMG concepts.

593 Finally, the maximum error made by averaging the prices of wood chips, methanol and natural gas in the
594 CHOP-reduced dataset was estimated for design B1. Two additional simulations were conducted: One for a
595 scenario where fuel prices in all hours were set to the maximum fuel price expected over the period, see
596 Table 7, and one where the fuel prices in all hours were set to the minimum fuel price expected. The NPV
597 result was reduced with 0.3 M€, or 0.03%, when fuel prices were set to the minimum expected values,
598 while it was increased by 0.5 M€, or 0.06%, when fuel prices were set to the maximum expected values. As
599 these variations are considered negligible, especially in comparison to the other sources of uncertainty
600 investigated, it is deemed acceptable to average the prices of wood chips, methanol and natural gas in the
601 CHOP method for the present case.

602 4. Discussion

603 In addition to the outcomes presented and discussed in Section 3, a number of uncertainties were not
604 accounted for in the analysis. These are shortly discussed below.

605 First of all, the surrogate models do not represent all process integration opportunities available. The
606 Rankine cycle is modelled as a single black box, not allowing for steam extraction within or between turbine
607 stages, which could otherwise be beneficial in order to extract steam as close to the required temperature
608 and pressure as possible and thereby minimizing exergy destruction of the heat transfer [23]. In addition,
609 exhaust gases from the gas turbine could be used as heat source for the Rankine cycle rather than directly
610 for district heating, thereby increasing the conversion efficiency further. Spare capacity in the waste
611 incineration may also allow for combustion of unreacted product gas, providing an additional usage
612 opportunity for this energy flow. In effect, the results of this study should, with respect to process
613 integration synergies, be regarded as a rough and conservative estimate of synergy potentials.

614 Regarding TCE calculations, emissions associated with power generation and consumption may as well be
615 regarded as conservative estimates as annually averaged power generation emissions were used. In
616 practice, it is expected that the share of renewables in the power producer mix would be higher during
617 periods of low power prices and lower during periods of high power prices. As the optimized FMG
618 operation causes the system to increase the power consumption and reduce the power generation in
619 periods with low power prices, and vice versa in periods with high power prices, it is expected that the
620 consumed power on average will have lower marginal CO₂ emissions while generated power is expected to
621 replace production with higher marginal CO₂ emissions. In effect, this trend would make the overall TCE of
622 the optimized designs smaller than what is calculated. However, in order to verify these considerations, an
623 assessment of the system impact from FMG operation needs to be conducted. This is recommended as a
624 topic for future research.

625 Opposed to this, the assumption that the wood chips are CO₂ neutral is optimistic as it implies an
626 assumption of zero emissions associated with the cultivation, harvesting, storing and transportation of the
627 biomass. In reality, it is expected that a certain level of CO₂ emission will be associated with the
628 consumption of wood pellets, especially if they are transported over significant distances. This impact
629 would increase the TCE of the optimized designs in the case study.

630 With respect to the energy system data applied, data for three reference years was used to estimate a
631 period of 20 years. As discussed in Section 3.2, uncertainties in operating conditions were found to have a
632 significant impact on the estimated FMG performance. This suggests that more detailed energy system
633 data should be used in future analyses of the system, and that it would be relevant to define additional
634 likely energy system scenarios in order to assess performance variations in response to likely operating
635 condition uncertainties further.

636 In terms of uncertainty analysis, it must be noted that the scenario analysis and interest rate uncertainties
637 were treated separately in the present work in order to assess the impacts of each of these uncertainties in
638 detail. In reality, combinations of these uncertainties may lead to larger performance variation spans than
639 the ones identified.

640 In the present work, the CHOP method was used for aggregating energy system data. Though advantageous
641 in several ways, the use of the CHOP method has some flaws, the largest being the fact that short-term
642 thermal and product storages cannot be considered in the optimization. In order to investigate if benefits
643 from operation shifting made possible by short-term storages would change the optimal design of the FMG

644 concept, it would be relevant to conduct the full design optimization using at least one additional data
645 aggregation method that allows for the inclusion of short-term storages.

646 Concerning the biorefinery, the two-stage gasifier was mathematically designed in the FMG to scale
647 between 5-200MW_{th} input. As mentioned, the gasifier has only been scaled up to 1.5MW_{th} in practice and
648 hence this projection is associated with some technological uncertainty. While regular downdraft gasifiers
649 usually scale up to 1-5MW_{th} [49,50], the two separate reactors in the two-stage gasifier allow some degrees
650 of freedom with regards to design. The gasification concept is therefore projected to scale well, with the
651 main challenges being the downdraft char gasifier and the externally heated pyrolysis unit. Replacing these
652 units with other more scalable reactors, such as updraft or fluid bed, could lead to an effective scaling of
653 the concept. For instance, Bentzen et al. [51] constructed an alternative and more scalable version of the
654 two-stage gasifier using two fluid beds for fuel processing. With activated carbon at room temperature as
655 the only downstream gas cleaning unit, a high gas quality was obtained with negligible tar levels.

656 Regarding the SOEC, the dimensioning was done *a priori* based on the largest feasible hydrogen addition in
657 the methanol synthesis. It was found that the full SOEC capacity was utilized for more than 98% of the time
658 in the reference scenario. However, in the design optimization the SOEC was by default installed in the
659 biorefinery. With the prices of wood chips and power considered, wood chips is almost always a cheaper
660 resource than power, making it economically attractive to increase the dimension of the gasifier rather
661 than investing in SOEC capacity for hydrogen-boosted methanol production. Hence, under the given
662 economic circumstances, hydrogen boosted methanol production is only considered attractive if wood chip
663 availability is limited, questioning if an SOEC with capacity for maximum hydrogen production should be
664 installed by default. Optimizing the dimension of the SOEC with respect to investment and operating
665 pattern would be a relevant topic for future research.

666 For the low fuel price scenario, the SOEC was operated in full capacity when power prices were below 66
667 €/MWh, equalling 79.0% of the operation duration. The SOEC was operated in oxygen-boosted mode for
668 power prices in the range 66 €/MWh to 122 €/MWh, approximately 20.9% of the time, while it was shut
669 down the last 0.1% of the time when power prices exceeded 122 €/MWh. Here, it could be relevant to
670 investigate the impact of including oxygen storage, which could allow the SOEC to be shut down for the
671 21% of the time where the power price is too high for operation in hydrogen-boosted mode. If feasible, it
672 could as well be considered if the SOEC operation could be inverted to make it run as a fuel cell on syngas
673 during periods of high power prices. If so, the SOEC could be used for storing electricity as methanol, and
674 then converting it to electricity when demands and prices are high, thereby extending the electricity system
675 balancing from the FMG. The possibility of running the SOEC as a fuel cell may as well serve as an option for
676 reducing the economic risk of low fuel prices for the overall FMG.

677 Finally, the middle estimated value of CO₂ emission quotas from ref. [42] was included in the methanol
678 price applied in the study. Over the period considered, the CO₂ emission quota value accounted for
679 between 2.5% and 11.5% of the methanol price depending on the year. In case the conservative estimate
680 of CO₂ emission quota value from ref. [42] had been used, the methanol price would have dropped
681 between 0.7% and 4.4% over the period, while the optimistic estimate would have let to increases in
682 methanol price of 0.0% to 4.5%. Such variations would have a noticeable impact on NPVs of the designs,
683 but the impact would fall within the NPV variation boundaries set by the $\pm 25\%$ change in methanol price
684 that was assessed as part of the uncertainty analysis.

685 5. Conclusion

686 The present study treated the development of a flexible multi-generation system (FMG) which integrated a
687 methanol-producing biorefinery with an existing CHP unit and industrial energy utility supply. Applying a
688 previously developed design methodology, the FMG was modelled and its design optimized with respect to
689 a 20-year system lifetime. Design aspects considered include: Process selection, dimensioning, location and
690 integration; operation optimization considering hourly variations in operating conditions over the year as
691 well as expected long term energy system development; and uncertainty analysis considering both
692 investment costs and operating conditions.

693 Solving the design optimization for the reference scenario, the outcomes suggest that the optimal design
694 with respect to both economic and environmental performance involved a maximum-sized biorefinery
695 located next to the local industry. As the local industry energy demands were limited when compared to
696 the biorefinery dimensions considered, process integration synergies were found to be marginal when
697 compared to the economic and environmental impact of the biorefinery. The results further indicated that
698 uncertainties in operating conditions, especially methanol price, would have a much higher impact on the
699 performance of the designs than corresponding uncertainties in investment costs.

700 For the optimized design, the net present value (NPV) was estimated to vary within the range 252.5 M€ to
701 1471.6 M€ in response to parameter value changes of $\pm 25\%$ of investments costs and methanol price. In
702 addition, a change in the applied interest rate from 5% to 20% in the reference scenario would reduce the
703 NPV to 181.3 M€. These significant variations in NPVs stress the importance of including systematic
704 uncertainty analysis in the design optimization of FMG concepts.

705 Acknowledgements

706 The authors would like to acknowledge DONG Energy, Energinet.dk, and the Innovation Foundation
707 through the 4DH project for their financial support of the research.

708 References

- 709 [1] Lund H. Renewable Energy Systems: The Choice and Modeling of 100% Renewable Solutions. Academic Press publications;
710 2010.
- 711 [2] Lund H, Andersen AN, Østergaard PA, Mathiesen BV, Connolly D. From electricity smart grids to smart energy systems - A
712 market operation based approach and understanding. *Energy* 2012;42:96–102. doi:10.1016/j.energy.2012.04.003.
- 713 [3] Mathiesen BV, Lund H, Connolly D, Wenzel H, Østergaard P a., Möller B, et al. Smart Energy Systems for coherent 100%
714 renewable energy and transport solutions. *Appl Energy* 2015;145:139–54. doi:10.1016/j.apenergy.2015.01.075.
- 715 [4] DTU. DTU International Energy Report 2015 : Energy systems integration for the transition to non-fossil energy systems
716 (http://www.natlab.dtu.dk/english/Energy_Reports/DIER-2015). 2015.
- 717 [5] Gassner M, Maréchal F. Thermo-economic optimisation of the polygeneration of synthetic natural gas (SNG), power and
718 heat from lignocellulosic biomass by gasification and methanation. *Energy Environ Sci* 2012;5:5768.
719 doi:10.1039/c1ee02867g.
- 720 [6] Lythcke-Jørgensen C, Ensinas A V., Münster M, Haglind F. A methodology for designing flexible multi-generation systems
721 (in press). *Energy* 2016:1–21.
- 722 [7] Liu P, Pistikopoulos EN, Li Z. Polygeneration Systems Engineering. *Process Syst. Eng.*, vol. 5, 2011, p. 1–38.
723 doi:10.1002/9783527631292.ch1.
- 724 [8] Chicco G, Mancarella P. Distributed multi-generation: A comprehensive view. *Renew Sustain Energy Rev* 2009;13:535–51.
725 doi:10.1016/j.rser.2007.11.014.
- 726 [9] Liu P, Pistikopoulos EN, Li Z. Decomposition Based Stochastic Programming Approach for Polygeneration Energy Systems

- 727 Design under Uncertainty. *Ind Eng Chem Res* 2010;49:3295–305. doi:10.1021/ie901490g.
- 728 [10] Maréchal F, Weber C, Favrat D. Multiobjective Design and Optimization of Urban Energy Systems. *Process Syst. Eng.*, 2011,
729 p. 39–83. doi:10.1002/9783527631292.ch1.
- 730 [11] Fazlollahi S, Becker G, Maréchal F. Multi-objectives, multi-period optimization of district energy systems: I. Selection of
731 typical operating periods. *Comput Chem Eng* 2014;65:54–66. doi:10.1016/j.compchemeng.2014.02.018.
- 732 [12] Fazlollahi S, Becker G, Maréchal F. Multi-objectives, multi-period optimization of district energy systems: II-Daily thermal
733 storage. *Comput Chem Eng* 2014;71:648–62. doi:10.1016/j.compchemeng.2014.02.018.
- 734 [13] Fazlollahi S, Becker G, Maréchal F. Multi-objectives, multi-period optimization of district energy systems: III. Distribution
735 networks. *Comput Chem Eng* 2014;66:82–97. doi:10.1016/j.compchemeng.2014.02.018.
- 736 [14] Sorknæs P, Lund H, Andersen AN. Future power market and sustainable energy solutions – The treatment of uncertainties
737 in the daily operation of combined heat and power plants. *Appl Energy* 2015;144:129–38.
738 doi:10.1016/j.apenergy.2015.02.041.
- 739 [15] Capuder T, Mancarella P. Techno-economic and environmental modelling and optimization of flexible distributed multi-
740 generation options. *Energy* 2014;71:516–33. doi:10.1016/j.energy.2014.04.097.
- 741 [16] Capuder T, Mancarella P. Modelling and Assessment of the Techno-economic and Environmental Performance of Flexible
742 Multi- Generation Systems. 18th Power Syst Comput Conf Wroclaw, Pol 2014.
- 743 [17] Martínez Ceseña E, Capuder T, Mancarella P. Flexible Distributed Multienergy Generation System Expansion Planning
744 Under Uncertainty. *IEEE Trans Smart Grid* 2015:1–10. doi:10.1109/TSG.2015.2411392.
- 745 [18] Piacentino A, Barbaro C, Cardona F, Gallea R, Cardona E. A comprehensive tool for efficient design and operation of
746 polygeneration-based energy micro-grids serving a cluster of buildings. Part I: Description of the method. *Appl Energy*
747 2013;111:1204–21. doi:10.1016/j.apenergy.2012.11.079.
- 748 [19] Zhou Z, Zhang J, Liu P, Li Z, Georgiadis MC, Pistikopoulos EN. A two-stage stochastic programming model for the optimal
749 design of distributed energy systems. *Appl Energy* 2013;103:135–44. doi:10.1016/j.apenergy.2012.09.019.
- 750 [20] Rubio-Maya C, Uche-Marcuello J, Martínez-Gracia A, Bayod-Rújula A a. Design optimization of a polygeneration plant
751 fuelled by natural gas and renewable energy sources. *Appl Energy* 2011;88:449–57. doi:10.1016/j.apenergy.2010.07.009.
- 752 [21] Chen Y, Adams TA, Barton PI. Optimal design and operation of flexible energy polygeneration systems. *Ind Eng Chem Res*
753 2011;50:4553–66. doi:10.1021/ie1021267.
- 754 [22] Lythcke-Jørgensen C, Haglind F, Clausen LR. Thermodynamic and Economic Analysis of Integrating Lignocellulosic
755 Bioethanol, Copenhagen, Denmark: European Biomass Conference and Exhibition; 2013, p. 1–8.
- 756 [23] Lythcke-Jørgensen C, Haglind F, Clausen LR. Exergy analysis of a combined heat and power plant with integrated
757 lignocellulosic ethanol production. *Energy Convers Manag* 2014;85:817–27. doi:10.1016/j.enconman.2014.01.018.
- 758 [24] Lythcke-Jørgensen C, Haglind F. Design optimization of a polygeneration plant producing power , heat , and lignocellulosic
759 ethanol. *Energy Convers Manag* 2015;91:353–66. doi:10.1016/j.enconman.2014.12.028.
- 760 [25] Lythcke-Jørgensen C, Münster M, Ensinas A V, Haglind F. Design optimization of flexible biomass-processing
761 polygeneration plants using characteristic operation periods. *World Renew. Energy Congr. XIII, London: 2014.*
- 762 [26] Danmarks Statistik 2014. <http://www.statistikbanken.dk/>.
- 763 [27] Thiessen K. Fjernvarme Horsens (personal contact) 2015. fjho.dk.
- 764 [28] Clausen LR, Elmegaard B, Ahrenfeldt J, Henriksen U. Thermodynamic analysis of small-scale dimethyl ether (DME) and
765 methanol plants based on the efficient two-stage gasifier. *Energy* 2011;36:5805–14. doi:10.1016/j.energy.2011.08.047.
- 766 [29] Clausen LR. Maximizing biofuel production in a thermochemical biorefinery by adding electrolytic hydrogen and by
767 integrating torrefaction with entrained flow gasification. *Energy* 2015;85:94–104. doi:10.1016/j.energy.2015.03.089.
- 768 [30] Lythcke-Jørgensen C, Haglind F, Ensinas A V., Münster M. A method for aggregating external operating conditions in multi-
769 generation plant optimization models. *Appl Energy* 2016:59–75. doi:10.1016/j.apenergy.2015.12.050.
- 770 [31] Energistyrelsen, Energinet.dk. Technology Data for Energy Plants - Generation of Electricity and District Heating, Energy
771 Storage and Energy Carrier Generation and Conversion 2015:1–220. doi:ISBN: 978-87-7844-940-5.
- 772 [32] Ahrenfeldt J, Henriksen U, Jensen TK, G??bel B, Wiese L, Kather A, et al. Validation of a continuous combined heat and
773 power (CHP) operation of a two-stage biomass gasifier. *Energy and Fuels* 2006;20:2672–80. doi:10.1021/ef0503616.
- 774 [33] Ahrenfeldt J, Thomsen TP, Henriksen U, Clausen LR. Biomass gasification cogeneration - A review of state of the art
775 technology and near future perspectives. *Appl Therm Eng* 2013;50:1407–17. doi:10.1016/j.applthermaleng.2011.12.040.
- 776 [34] Evald A, Hu G, Hansen MT. Technology data for advanced bioenergy fuels. 2013.
- 777 [35] Vad Mathiesen B, Ridjan I. Technology Data for High Temperature Solid Oxide Electrolyser Cells , Alkali and Pem
778 Electrolysers. Aalborg, Denmark: 2013.
- 779 [36] Jensen JK, Ommen T, Markussen WB, Reinholdt L, Elmegaard B. Technical and economic working domains of industrial

780 heat pumps: Part 2 - Ammonia-water hybrid absorption-compression heat pumps. *Int J Refrig* 2014;55:183–200.
781 doi:10.1016/j.ijrefrig.2015.02.011.

782 [37] Dansk Fjernvarme. Temamøde om landsbyvarme 2015. <http://www.danskfjernvarme.dk/kurser-og->
783 [moeder/moedematerialer/2014-25-marts-temamoede-om-landsbynaerva](http://www.danskfjernvarme.dk/kurser-og-moeder/moedematerialer/2014-25-marts-temamoede-om-landsbynaerva) (accessed March 31, 2016).

784 [38] Energiforskning.dk. Analyser for kommercialisering af brintteknologier n.d.
785 <http://www.energiforskning.dk/da/project/analyser-kommercialisering-af-brintteknologier> (accessed March 15, 2016).

786 [39] Danish Energy Agency. FORUDSÆTNINGER FOR SAMFUNDSØKONOMISKE ANALYSER PÅ ENERGIOMRÅDET. 2014.

787 [40] Danish Energy Agency. Oliepriser 2016. <http://www.ens.dk/info/tal-kort/statistik-nogleletal/energipriser-afgifter/oliepriser>
788 (accessed March 29, 2016).

789 [41] Energinet.dk. SIFRE: Simulation of Flexible and Renewable Energy sources
790 (http://energinet.dk/SiteCollectionDocuments/Danske%20dokumenter/El/sifre_fall2015.pdf). 2015.

791 [42] Energinet.dk. Energinet.dk's analyseforudsætninger 2012-2035. 2012.

792 [43] Energinet.dk, Dansk Energi. Smart Energy - hovedrapport ([http://energinet.dk/DA/KLIMA-OG-](http://energinet.dk/DA/KLIMA-OG-MILJØE/Energianalyser/Analyser/Sider/Smart-Energy.aspx)
793 [MILJØE/Energianalyser/Analyser/Sider/Smart-Energy.aspx](http://energinet.dk/DA/KLIMA-OG-MILJØE/Energianalyser/Analyser/Sider/Smart-Energy.aspx)) 2015.

794 [44] Energistyrelsen. Energistatistik 2014 – Data, tabeller, statistikker og kort. 2015.

795 [45] Turton R, Bailie RC, Whiting WB, Shaeiwitz J a. *Analysis, Synthesis, and Design of Chemical Processes*. 1998.

796 [46] Bolliger R. *Méthodologie de la synthèse des systèmes énergétiques industriels*. 2010. doi:10.5075/epfl-thesis-4867.

797 [47] Sin G, Gernaey K V., Lantz AE. Good modeling practice for PAT applications: Propagation of input uncertainty and
798 sensitivity analysis. *Biotechnol. Prog.*, vol. 25, 2009, p. 1043–53. doi:10.1002/btpr.166.

799 [48] McKay MD, Beckman RJ, Conover WJ. Comparison of three methods for selecting values of input variables in the analysis
800 of output from a computer code. *Technometrics* 1979;21:239–45. doi:10.2307/1271432.

801 [49] Basu P. *Biomass Gasification, Pyrolysis and Torrefaction*. 2013. doi:10.1016/B978-0-12-396488-5.00013-7.

802 [50] Knoef H. *Handbook Biomass Gasification*. Biomass Gasification Group; 2005.

803 [51] Bentzen J, Hummelshøj R, Henriksen U. Upscale of the two-stage gasification process. *Proc 2 World Conf Technol Exhib*
804 *Biomass Energy Ind* 2004;10-14 May,:1004–7.

805 [52] Adams TA, Ghouse JH. Polygeneration of fuels and chemicals. *Curr Opin Chem Eng* 2015;10:87–93.
806 doi:10.1016/j.coche.2015.09.006.

807

808 **Appendix A – System model data**

809 This appendix includes all mass and energy flow functions of the FMG system model.

810 **Table 12: Thermal energy flow functions.**

Facility	Flow-description	Notation	Type	Function [MJ/s]	T_{in}/T_{out}
Horsens CHP	0.8 bar condenser heat	$\dot{Q}_{ran,hp}$	Hot	$\lambda_{ran}\dot{Q}_{ran,hp0}$	93.5°C / 93.5°C
	0.3 bar condenser heat	$\dot{Q}_{ran,lp}$	Hot	$\lambda_{ran}\dot{Q}_{ran,lp0}$	69.1°C / 69.1°C
	Gas turbine, off gas heat	$\dot{Q}_{gt,off}$	Hot	$\lambda_{gt}\sigma_{gt}(\eta_{gt} - \eta_{gt,P})$	600°C / 70°C
	District heating generation	\dot{Q}_{dh}	Cold	$\sigma_{dh}\lambda_{dh}$	40°C / 90°C
Butchery	Room heating and losses	$\dot{Q}_{ind,room}$	Cold	$0.24 \cdot \sigma_{ind}\lambda_{ind}$	35°C / 35°C
	Cleaning	$\dot{Q}_{ind,cl}$	Cold	$0.37 \cdot \sigma_{ind}\lambda_{ind}$	
	Boiling and evaporation	$\dot{Q}_{ind,ev}$	Cold	$0.04 \cdot \sigma_{ind}\lambda_{ind}$	110°C / 100°C
	Gas boiler, off gas heat	$\dot{Q}_{gb,off}$	Hot	$\sigma_{ind}\lambda_{gb,ind}$	1000°C / 70°C
Hybrid heat pump	District heating source	$\dot{Q}_{hp,in}$	Cold	$\sigma_{hp}\lambda_{hp} \frac{COP - 1}{COP}$	40°C / 90°C
	Process heat sink	$\dot{Q}_{hp,out}$	Hot	$\sigma_{hp}\lambda_{hp}$	120°C / 110°C
Biorefinery	Gasifier, B	\dot{Q}_B	Cold	$0.118 \cdot \sigma_{bio}$	115°C / 200°C
	Gasifier, C	\dot{Q}_C	Hot	$0.020 \cdot \sigma_{bio}$	236°C / 127°C
	Gasifier, D	\dot{Q}_D	Hot	$0.062 \cdot \sigma_{bio}$	114°C / 40°C
	Methanol, G	\dot{Q}_G	Hot	$0.070 \cdot \sigma_{bio}\lambda_{meth}$	220°C / 220°C
	Methanol, H	\dot{Q}_H	Hot	$0.076 \cdot \sigma_{bio}\lambda_{meth}$	110°C / 40°C
	Methanol, J	\dot{Q}_J	Cold	$0.010 \cdot \sigma_{bio}\lambda_{meth}$	84°C / 84°C
	Methanol, K	\dot{Q}_K	Cold	$0.033 \cdot \sigma_{bio}\lambda_{meth}$	40°C / 110°C
	Methanol, N	\dot{Q}_K	Hot	$0.122 \cdot \sigma_{bio}\lambda_{meth}$	153°C / 40°C
	SOEC excess heat	\dot{Q}_K	Hot	$0.5 \cdot \sigma_{bio}\lambda_{soec} \left(\frac{1 - \eta_{SOEC}}{\eta_{SOEC}} \right)$	200°C / 40°C
	Off-product gas burner	\dot{Q}_{off}	Hot	$0.24 \cdot \sigma_{bio} \cdot \lambda_{sb}$	600°C / 70°C

811 **Table 13: Energy flow functions.**

Process	Flow-description	Notation	Function [MW]
WOOD CHIPS FLOWS			
Biorefinery	Gasifier wood chip consumption	$\dot{e}_{wood\ chips}$	σ_{bio}
POWER FLOWS			
Horsens CHP	Power generation, Rankine	P_{ran}	$7 \cdot \lambda_{ran}$
	Power generation, gas turbine	P_{gt}	$8 \cdot \lambda_{ran}$
Butchery	Ammonia-water hybrid heat pump	P_{hp}	$-\frac{\sigma_{hp}\lambda_{hp}}{COP}$
Biorefinery	Methanol production power demand	P_{meth}	$0.096 \cdot \lambda_{meth}\sigma_{bio}$
	SOEC power demand	P_{SOEC}	$\lambda_{SOEC} \frac{0.5 \cdot \sigma_{bio}}{\eta_{SOEC}}$
NATURAL GAS FLOWS			

Horsens CHP	Gas turbine natural gas consumption	$\dot{e}_{ng,gt}$	$\sigma_{gt} \cdot \lambda_{gt}$
Butchery	Gas boiler natural gas consumption	$\dot{e}_{ng,gb}$	$\sigma_{ind} \lambda_{gb} (0.35 + \beta_{ng})$
PRODUCT GAS and OFF-PRODUCT GAS FLOWS			
Biorefinery	Gasifier, product gas generation	\dot{e}_{syngas}	$0.9294 \cdot \sigma_{bio}$
	Methanol off-product gas, air blown	$\dot{e}_{synoff,air}$	$0.24 \cdot \sigma_{bio} \lambda_{meth}$
	Methanol off-product gas, oxygen blown	\dot{e}_{synoff,O_2}	$0.02 \cdot \sigma_{bio} \lambda_{meth}$
Butchery	Gas boiler off-product gas consumption	$\dot{e}_{synoff,gb}$	$\sigma_{ind} \lambda_{gb} (1 - \beta_{ng})$
HYDROGEN FLOWS			
Biorefinery	Hydrogen, SOEC	$\dot{e}_{H_2,SOEC}$	$0.5 \cdot \lambda_{SOEC} \sigma_{bio}$
	Hydrogen addition, oxygen-blown	\dot{e}_{H_2,O_2}	$0.184 \cdot \lambda_{MeOH,O_2} \sigma_{bio}$
	Hydrogen addition, hydrogen-boost	\dot{e}_{MeOH,H_2+}	$0.316 \cdot \lambda_{MeOH,H_2+} \sigma_{bio}$
METHANOL FLOWS			
Biorefinery	Methanol, air-blown	$\dot{e}_{MeOH,air}$	$0.56 \cdot \lambda_{MeOH,air} \sigma_{bio}$
	Additional methanol, oxygen-blown	\dot{e}_{MeOH,O_2}	$0.34 \cdot \lambda_{MeOH,O_2} \sigma_{bio}$
	Additional methanol, hydrogen-boost	\dot{e}_{MeOH,H_2+}	$0.32 \cdot \lambda_{MeOH,H_2+} \sigma_{bio}$

812

Table 14: Mass flow functions.

Process	Flow-description	Notation	Function [MW]
WASTE FLOWS			
Horsens CHP	Waste incineration boilers waste processing	$\dot{m}_{waste,ran}$	$\sigma_{ran} \cdot \lambda_{ran}$
OXYGEN FLOWS			
Biorefinery	SOEC, oxygen production	$\dot{m}_{O_2,SOEC}$	$0.0337 \cdot \sigma_{bio} \lambda_{SOEC}$
	Gasifier, oxygen-blown	$\dot{m}_{O_2,gasifier}$	$0.0124 \cdot \sigma_{bio} \lambda_{O_2-blown}$

813

814

815 Appendix B – CHOP-reduction of external operating condition data

816 This appendix describes the applied data aggregation procedure using the CHOP method [30].

817 Through an iterative assessment, it was decided to define six important parameter intervals for the power
818 price, five important parameter intervals for the district heating demand, and four important parameter
819 intervals for the industry utility demand. The applied interval break points are presented in Table 15.

820 The break points for relative district heating demand and relative thermal utility demand in the industry
821 were defined based on the duration curves. The power price break points were identified iteratively by
822 optimizing the operation of the developed model for various price schemes. Using the present-value-
823 averaged methanol price and natural gas price, it was found that Rankine power generation was shifted
824 from minimum to maximum when the power price exceeded approximately 75.00 Euro/MWh. Similarly,
825 the gas turbine power generation was maximized when power prices were around 92.00 Euro/MWh or
826 higher, while SOEC loads were reduced to operation in oxygen-blown mode when power prices were above
827 90.00 Euro/MWh. For power prices above 146.00 Euro/MWh, the SOEC was found to shut down, but such
828 high power prices were only present in 6 hours over the entire 20-year period reference dataset, hence it
829 was not deemed relevant to add a break point at this value.

830 **Table 15: Interval break points used in the CHOP reduction of volatile external operating conditions parameters in the case study.**

Interval number	Power price, break point [Euro/MWh]	Relative District heating demand, break point [-]	Industry relative thermal utility demand, break point [-]
1	20.00	0.25	0.20
2	40.00	0.40	0.50
3	60.00	0.60	0.80
4	75.00	0.80	1.00
5	90.00	1.00	
6	152.53		

831 Using the interval break points in Table 15, the resulting CHOP reduced dataset of the reference scenario is
832 presented in Table 16. The CHOP reduced dataset for the reference scenario when an interest rate of 20%
833 was applied is presented in Table 17: CHOP dataset of the reference scenario when an interest rate of 20%
834 was used for calculating the present value factors t_{pv} . Table 17, while the CHOP reduced dataset of the
835 NonFlex scenario is presented in Table 18.

836 **Table 16: CHOP dataset of the reference scenario used in the study. Notice that CHOP groups with durations of 0 are so-called**
837 **'empty' CHOP groups, meaning that no reference operating point falls within the group boundaries. Empty CHOP-groups are**
838 **discarded from the final CHOP dataset and are grey-shaded in the table.**

Group (p,d,i)	t [h]	t_{pv}	c_p [€/MWh]	α_p [T/MWh]	λ_{DH}	λ_{ind}	c_{MeOH} [€/GJ]	c_{NG} [€/GJ]	c_{wood} [€/GJ]
(1,1,1)	1524	1262	16.24	263	0.19	0.13	21.42	9.68	6.54
(1,1,2)	1680	1215	16.14	243	0.18	0.36	22.48	9.81	6.69
(1,1,3)	222	130	14.27	198	0.19	0.58	24.47	10.05	6.97
(1,1,4)	0	0	0.00	0	0.00	0.00	0.00	0.00	0.00
(1,2,1)	356	293	14.63	260	0.31	0.12	21.47	9.68	6.54
(1,2,2)	556	358	13.50	217	0.30	0.36	23.52	9.93	6.84

(1,2,3)	202	119	11.76	193	0.32	0.58	24.42	10.03	6.96
(1,2,4)	6	5	15.30	270	0.32	0.86	21.25	9.66	6.52
(1,3,1)	848	617	13.40	243	0.49	0.15	22.42	9.80	6.68
(1,3,2)	1494	912	12.45	208	0.51	0.38	24.04	9.99	6.91
(1,3,3)	636	332	9.72	170	0.51	0.61	25.74	10.20	7.15
(1,3,4)	42	23	11.23	182	0.51	0.83	25.21	10.13	7.08
(1,4,1)	494	381	14.65	253	0.67	0.16	21.96	9.74	6.62
(1,4,2)	992	792	16.14	260	0.71	0.36	21.68	9.71	6.58
(1,4,3)	270	206	17.36	252	0.72	0.57	22.04	9.76	6.63
(1,4,4)	0	0	0.00	0	0.00	0.00	0.00	0.00	0.00
(1,5,1)	138	117	17.15	270	0.89	0.17	21.25	9.66	6.52
(1,5,2)	270	228	16.72	270	0.87	0.31	21.25	9.66	6.52
(1,5,3)	42	36	18.51	270	0.86	0.56	21.25	9.66	6.52
(1,5,4)	0	0	0.00	0	0.00	0.00	0.00	0.00	0.00
(2,1,1)	7572	5513	29.44	210	0.19	0.12	22.59	9.77	6.67
(2,1,2)	11940	9098	28.41	244	0.19	0.36	22.09	9.75	6.63
(2,1,3)	2438	1874	30.65	249	0.21	0.58	22.00	9.74	6.62
(2,1,4)	24	20	30.51	270	0.19	0.82	21.25	9.66	6.52
(2,2,1)	2028	1442	29.67	210	0.32	0.13	22.77	9.80	6.70
(2,2,2)	2984	2290	28.64	247	0.32	0.37	22.02	9.74	6.62
(2,2,3)	992	753	30.90	247	0.31	0.58	22.10	9.76	6.64
(2,2,4)	6	3	33.30	112	0.25	0.86	28.34	10.51	7.52
(2,3,1)	3500	2606	29.17	223	0.49	0.15	22.36	9.76	6.65
(2,3,2)	6994	5419	29.16	246	0.49	0.37	21.96	9.73	6.61
(2,3,3)	2958	2273	32.31	248	0.51	0.61	22.01	9.74	6.62
(2,3,4)	48	38	29.84	259	0.53	0.83	21.73	9.72	6.59
(2,4,1)	3638	2756	30.29	231	0.70	0.17	22.19	9.74	6.63
(2,4,2)	6526	5111	29.41	247	0.70	0.37	21.88	9.72	6.60
(2,4,3)	4162	3337	30.09	258	0.70	0.61	21.67	9.70	6.57
(2,4,4)	216	173	31.83	261	0.72	0.85	21.67	9.71	6.58
(2,5,1)	768	615	30.01	248	0.86	0.17	21.73	9.70	6.57
(2,5,2)	2052	1689	29.00	259	0.87	0.37	21.48	9.68	6.55
(2,5,3)	1460	1233	29.23	269	0.86	0.61	21.26	9.66	6.52
(2,5,4)	90	76	31.93	270	0.82	0.84	21.25	9.66	6.52
(3,1,1)	6834	3653	49.07	113	0.18	0.13	25.78	10.11	7.09
(3,1,2)	13388	7306	49.63	116	0.17	0.36	25.55	10.08	7.06
(3,1,3)	2304	1275	49.59	131	0.20	0.58	25.35	10.07	7.04
(3,1,4)	30	20	50.80	153	0.18	0.82	23.75	9.86	6.80
(3,2,1)	2100	1098	50.79	113	0.34	0.14	26.01	10.15	7.13
(3,2,2)	4458	2361	51.59	115	0.34	0.37	25.86	10.13	7.11
(3,2,3)	762	382	49.94	131	0.33	0.58	26.37	10.23	7.21
(3,2,4)	0	0	0.00	0	0.00	0.00	0.00	0.00	0.00
(3,3,1)	2492	1375	50.74	114	0.49	0.15	25.45	10.06	7.04

(3,3,2)	5848	3139	51.33	113	0.50	0.38	25.74	10.10	7.09
(3,3,3)	2272	1154	50.41	118	0.52	0.59	26.29	10.20	7.18
(3,3,4)	80	43	46.97	168	0.51	0.84	25.42	10.14	7.10
(3,4,1)	1956	1098	48.42	117	0.69	0.17	25.27	10.04	7.01
(3,4,2)	4692	2657	49.74	120	0.69	0.35	25.17	10.03	7.00
(3,4,3)	2892	1663	50.07	124	0.69	0.60	25.01	10.01	6.98
(3,4,4)	126	77	46.52	174	0.71	0.86	24.16	9.96	6.89
(3,5,1)	192	116	49.07	112	0.86	0.17	24.63	9.93	6.90
(3,5,2)	634	410	47.10	149	0.85	0.37	23.83	9.87	6.81
(3,5,3)	366	245	46.95	168	0.86	0.62	23.44	9.84	6.77
(3,5,4)	0	0	0.00	0	0.00	0.00	0.00	0.00	0.00
(4,1,1)	2492	1146	65.06	112	0.17	0.13	27.43	10.37	7.37
(4,1,2)	7348	3821	65.38	112	0.18	0.37	26.07	10.15	7.14
(4,1,3)	2000	1071	66.46	112	0.19	0.58	25.77	10.11	7.09
(4,1,4)	32	15	64.99	112	0.17	0.82	27.15	10.32	7.32
(4,2,1)	1030	468	65.13	112	0.34	0.15	27.58	10.39	7.39
(4,2,2)	2844	1384	65.21	112	0.34	0.37	26.79	10.27	7.26
(4,2,3)	890	466	65.29	112	0.33	0.59	26.00	10.14	7.13
(4,2,4)	0	0	0.00	0	0.00	0.00	0.00	0.00	0.00
(4,3,1)	2202	1084	65.10	112	0.50	0.16	26.66	10.25	7.24
(4,3,2)	5302	2782	66.48	112	0.49	0.37	25.97	10.14	7.12
(4,3,3)	3496	1846	67.49	112	0.50	0.61	25.91	10.13	7.11
(4,3,4)	188	94	68.17	112	0.51	0.83	26.44	10.21	7.20
(4,4,1)	1318	730	67.74	112	0.68	0.17	25.42	10.05	7.03
(4,4,2)	3520	1979	67.66	112	0.69	0.36	25.28	10.03	7.01
(4,4,3)	3192	1768	68.52	112	0.68	0.63	25.43	10.05	7.03
(4,4,4)	208	117	68.98	112	0.69	0.85	25.28	10.03	7.01
(4,5,1)	192	116	64.98	112	0.85	0.16	24.63	9.93	6.90
(4,5,2)	576	347	66.38	112	0.86	0.34	24.63	9.93	6.90
(4,5,3)	160	96	65.58	112	0.89	0.60	24.63	9.93	6.90
(4,5,4)	0	0	0.00	0	0.00	0.00	0.00	0.00	0.00
(5,1,1)	1194	519	81.66	112	0.16	0.13	28.13	10.48	7.49
(5,1,2)	2538	1287	80.69	112	0.19	0.37	26.34	10.20	7.19
(5,1,3)	1172	616	80.61	112	0.20	0.59	25.96	10.14	7.12
(5,1,4)	0	0	0.00	0	0.00	0.00	0.00	0.00	0.00
(5,2,1)	360	154	80.82	112	0.34	0.14	28.34	10.51	7.52
(5,2,2)	952	452	80.20	112	0.35	0.37	27.07	10.31	7.31
(5,2,3)	640	314	80.84	112	0.34	0.62	26.69	10.25	7.24
(5,2,4)	12	5	78.33	112	0.37	0.82	28.34	10.51	7.52
(5,3,1)	572	246	82.40	112	0.51	0.16	28.27	10.50	7.51
(5,3,2)	1526	776	80.04	112	0.49	0.37	26.31	10.19	7.18
(5,3,3)	1394	736	79.44	112	0.48	0.63	25.91	10.13	7.11
(5,3,4)	72	35	81.81	112	0.52	0.84	26.81	10.27	7.26

(5,4,1)	296	157	79.74	112	0.68	0.18	25.84	10.12	7.10
(5,4,2)	1504	835	78.80	112	0.69	0.39	25.40	10.05	7.03
(5,4,3)	1842	1044	78.91	112	0.70	0.63	25.20	10.02	7.00
(5,4,4)	206	123	78.23	112	0.70	0.85	24.71	9.94	6.91
(5,5,1)	0	0	0.00	0	0.00	0.00	0.00	0.00	0.00
(5,5,2)	104	63	75.71	112	0.85	0.36	24.63	9.93	6.90
(5,5,3)	0	0	0.00	0	0.00	0.00	0.00	0.00	0.00
(5,5,4)	0	0	0.00	0	0.00	0.00	0.00	0.00	0.00
(6,1,1)	234	100	120.30	112	0.16	0.12	28.34	10.51	7.52
(6,1,2)	396	186	117.19	112	0.17	0.38	27.19	10.33	7.33
(6,1,3)	92	45	125.05	112	0.19	0.61	26.75	10.26	7.25
(6,1,4)	14	7	113.04	112	0.20	0.83	25.92	10.13	7.12
(6,2,1)	90	38	133.66	112	0.33	0.14	28.34	10.51	7.52
(6,2,2)	188	82	114.44	112	0.35	0.33	28.12	10.48	7.48
(6,2,3)	100	46	121.10	112	0.36	0.61	27.55	10.39	7.39
(6,2,4)	8	5	139.60	112	0.30	0.86	24.63	9.93	6.90
(6,3,1)	66	28	116.32	112	0.49	0.16	28.34	10.51	7.52
(6,3,2)	242	126	115.62	112	0.50	0.39	26.07	10.15	7.14
(6,3,3)	110	57	105.12	112	0.48	0.65	26.14	10.17	7.15
(6,3,4)	6	3	134.45	112	0.46	0.89	28.34	10.51	7.52
(6,4,1)	74	37	116.66	112	0.66	0.16	26.42	10.21	7.20
(6,4,2)	472	234	111.87	112	0.67	0.40	26.58	10.24	7.23
(6,4,3)	134	63	101.75	112	0.67	0.60	27.20	10.33	7.33
(6,4,4)	6	3	99.18	112	0.61	0.81	28.34	10.51	7.52
(6,5,1)	0	0	0.00	0	0.00	0.00	0.00	0.00	0.00
(6,5,2)	0	0	0.00	0	0.00	0.00	0.00	0.00	0.00
(6,5,3)	0	0	0.00	0	0.00	0.00	0.00	0.00	0.00
(6,5,4)	0	0	0.00	0	0.00	0.00	0.00	0.00	0.00

839
840

Table 17: CHOP dataset of the reference scenario when an interest rate of 20% was used for calculating the present value factors t_{pv} .

Group (p,d,i)	t [h]	t_{pv}	c_p [€/MWh]	α_p [T/MWh]	λ_{DH}	λ_{ind}	c_{MeOH} [€/GJ]	c_{NG} [€/GJ]	c_{wood} [€/GJ]
(1,1,1)	1524	804	16.24	263	0.19	0.13	21.42	9.68	6.54
(1,1,2)	1680	680	16.14	243	0.18	0.36	22.48	9.81	6.69
(1,1,3)	222	53	14.27	198	0.19	0.58	24.47	10.05	6.97
(1,1,4)	0	0	0.00	0	0.00	0.00	0.00	0.00	0.00
(1,2,1)	356	185	14.63	260	0.31	0.12	21.47	9.68	6.54
(1,2,2)	556	170	13.50	217	0.30	0.36	23.52	9.93	6.84
(1,2,3)	202	47	11.76	193	0.32	0.58	24.42	10.03	6.96
(1,2,4)	6	3	15.30	270	0.32	0.86	21.25	9.66	6.52
(1,3,1)	848	347	13.40	243	0.49	0.15	22.42	9.80	6.68
(1,3,2)	1494	399	12.45	208	0.51	0.38	24.04	9.99	6.91

(1,3,3)	636	101	9.72	170	0.51	0.61	25.74	10.20	7.15
(1,3,4)	42	8	11.23	182	0.51	0.83	25.21	10.13	7.08
(1,4,1)	494	228	14.65	253	0.67	0.16	21.96	9.74	6.62
(1,4,2)	992	491	16.14	260	0.71	0.36	21.68	9.71	6.58
(1,4,3)	270	122	17.36	252	0.72	0.57	22.04	9.76	6.63
(1,4,4)	0	0	0.00	0	0.00	0.00	0.00	0.00	0.00
(1,5,1)	138	76	17.15	270	0.89	0.17	21.25	9.66	6.52
(1,5,2)	270	150	16.72	270	0.87	0.31	21.25	9.66	6.52
(1,5,3)	42	23	18.51	270	0.86	0.56	21.25	9.66	6.52
(1,5,4)	0	0	0.00	0	0.00	0.00	0.00	0.00	0.00
(2,1,1)	7572	2789	29.44	210	0.19	0.12	22.59	9.77	6.67
(2,1,2)	11940	5257	28.41	244	0.19	0.36	22.09	9.75	6.63
(2,1,3)	2438	1104	30.65	249	0.21	0.58	22.00	9.74	6.62
(2,1,4)	24	13	30.51	270	0.19	0.82	21.25	9.66	6.52
(2,2,1)	2028	718	29.67	210	0.32	0.13	22.77	9.80	6.70
(2,2,2)	2984	1341	28.64	247	0.32	0.37	22.02	9.74	6.62
(2,2,3)	992	439	30.90	247	0.31	0.58	22.10	9.76	6.64
(2,2,4)	6	0	33.30	112	0.25	0.86	28.34	10.51	7.52
(2,3,1)	3500	1394	29.17	223	0.49	0.15	22.36	9.76	6.65
(2,3,2)	6994	3184	29.16	246	0.49	0.37	21.96	9.73	6.61
(2,3,3)	2958	1336	32.31	248	0.51	0.61	22.01	9.74	6.62
(2,3,4)	48	24	29.84	259	0.53	0.83	21.73	9.72	6.59
(2,4,1)	3638	1528	30.29	231	0.70	0.17	22.19	9.74	6.63
(2,4,2)	6526	3031	29.41	247	0.70	0.37	21.88	9.72	6.60
(2,4,3)	4162	2062	30.09	258	0.70	0.61	21.67	9.70	6.57
(2,4,4)	216	107	31.83	261	0.72	0.85	21.67	9.71	6.58
(2,5,1)	768	369	30.01	248	0.86	0.17	21.73	9.70	6.57
(2,5,2)	2052	1062	29.00	259	0.87	0.37	21.48	9.68	6.55
(2,5,3)	1460	806	29.23	269	0.86	0.61	21.26	9.66	6.52
(2,5,4)	90	50	31.93	270	0.82	0.84	21.25	9.66	6.52
(3,1,1)	6834	792	49.07	113	0.18	0.13	25.78	10.11	7.09
(3,1,2)	13388	1694	49.63	116	0.17	0.36	25.55	10.08	7.06
(3,1,3)	2304	335	49.59	131	0.20	0.58	25.35	10.07	7.04
(3,1,4)	30	7	50.80	153	0.18	0.82	23.75	9.86	6.80
(3,2,1)	2100	226	50.79	113	0.34	0.14	26.01	10.15	7.13
(3,2,2)	4458	510	51.59	115	0.34	0.37	25.86	10.13	7.11
(3,2,3)	762	83	49.94	131	0.33	0.58	26.37	10.23	7.21
(3,2,4)	0	0	0.00	0	0.00	0.00	0.00	0.00	0.00
(3,3,1)	2492	321	50.74	114	0.49	0.15	25.45	10.06	7.04
(3,3,2)	5848	687	51.33	113	0.50	0.38	25.74	10.10	7.09
(3,3,3)	2272	232	50.41	118	0.52	0.59	26.29	10.20	7.18
(3,3,4)	80	14	46.97	168	0.51	0.84	25.42	10.14	7.10
(3,4,1)	1956	269	48.42	117	0.69	0.17	25.27	10.04	7.01

(3,4,2)	4692	677	49.74	120	0.69	0.35	25.17	10.03	7.00
(3,4,3)	2892	444	50.07	124	0.69	0.60	25.01	10.01	6.98
(3,4,4)	126	29	46.52	174	0.71	0.86	24.16	9.96	6.89
(3,5,1)	192	31	49.07	112	0.86	0.17	24.63	9.93	6.90
(3,5,2)	634	147	47.10	149	0.85	0.37	23.83	9.87	6.81
(3,5,3)	366	99	46.95	168	0.86	0.62	23.44	9.84	6.77
(3,5,4)	0	0	0.00	0	0.00	0.00	0.00	0.00	0.00
(4,1,1)	2492	162	65.06	112	0.17	0.13	27.43	10.37	7.37
(4,1,2)	7348	773	65.38	112	0.18	0.37	26.07	10.15	7.14
(4,1,3)	2000	231	66.46	112	0.19	0.58	25.77	10.11	7.09
(4,1,4)	32	2	64.99	112	0.17	0.82	27.15	10.32	7.32
(4,2,1)	1030	63	65.13	112	0.34	0.15	27.58	10.39	7.39
(4,2,2)	2844	236	65.21	112	0.34	0.37	26.79	10.27	7.26
(4,2,3)	890	96	65.29	112	0.33	0.59	26.00	10.14	7.13
(4,2,4)	0	0	0.00	0	0.00	0.00	0.00	0.00	0.00
(4,3,1)	2202	191	65.10	112	0.50	0.16	26.66	10.25	7.24
(4,3,2)	5302	575	66.48	112	0.49	0.37	25.97	10.14	7.12
(4,3,3)	3496	387	67.49	112	0.50	0.61	25.91	10.13	7.11
(4,3,4)	188	18	68.17	112	0.51	0.83	26.44	10.21	7.20
(4,4,1)	1318	169	67.74	112	0.68	0.17	25.42	10.05	7.03
(4,4,2)	3520	470	67.66	112	0.69	0.36	25.28	10.03	7.01
(4,4,3)	3192	408	68.52	112	0.68	0.63	25.43	10.05	7.03
(4,4,4)	208	28	68.98	112	0.69	0.85	25.28	10.03	7.01
(4,5,1)	192	31	64.98	112	0.85	0.16	24.63	9.93	6.90
(4,5,2)	576	93	66.38	112	0.86	0.34	24.63	9.93	6.90
(4,5,3)	160	26	65.58	112	0.89	0.60	24.63	9.93	6.90
(4,5,4)	0	0	0.00	0	0.00	0.00	0.00	0.00	0.00
(5,1,1)	1194	57	81.66	112	0.16	0.13	28.13	10.48	7.49
(5,1,2)	2538	245	80.69	112	0.19	0.37	26.34	10.20	7.19
(5,1,3)	1172	128	80.61	112	0.20	0.59	25.96	10.14	7.12
(5,1,4)	0	0	0.00	0	0.00	0.00	0.00	0.00	0.00
(5,2,1)	360	16	80.82	112	0.34	0.14	28.34	10.51	7.52
(5,2,2)	952	71	80.20	112	0.35	0.37	27.07	10.31	7.31
(5,2,3)	640	55	80.84	112	0.34	0.62	26.69	10.25	7.24
(5,2,4)	12	1	78.33	112	0.37	0.82	28.34	10.51	7.52
(5,3,1)	572	26	82.40	112	0.51	0.16	28.27	10.50	7.51
(5,3,2)	1526	149	80.04	112	0.49	0.37	26.31	10.19	7.18
(5,3,3)	1394	154	79.44	112	0.48	0.63	25.91	10.13	7.11
(5,3,4)	72	6	81.81	112	0.52	0.84	26.81	10.27	7.26
(5,4,1)	296	33	79.74	112	0.68	0.18	25.84	10.12	7.10
(5,4,2)	1504	194	78.80	112	0.69	0.39	25.40	10.05	7.03
(5,4,3)	1842	251	78.91	112	0.70	0.63	25.20	10.02	7.00
(5,4,4)	206	32	78.23	112	0.70	0.85	24.71	9.94	6.91

(5,5,1)	0	0	0.00	0	0.00	0.00	0.00	0.00	0.00
(5,5,2)	104	17	75.71	112	0.85	0.36	24.63	9.93	6.90
(5,5,3)	0	0	0.00	0	0.00	0.00	0.00	0.00	0.00
(5,5,4)	0	0	0.00	0	0.00	0.00	0.00	0.00	0.00
(6,1,1)	234	10	120.30	112	0.16	0.12	28.34	10.51	7.52
(6,1,2)	396	28	117.19	112	0.17	0.38	27.19	10.33	7.33
(6,1,3)	92	8	125.05	112	0.19	0.61	26.75	10.26	7.25
(6,1,4)	14	2	113.04	112	0.20	0.83	25.92	10.13	7.12
(6,2,1)	90	4	133.66	112	0.33	0.14	28.34	10.51	7.52
(6,2,2)	188	9	114.44	112	0.35	0.33	28.12	10.48	7.48
(6,2,3)	100	6	121.10	112	0.36	0.61	27.55	10.39	7.39
(6,2,4)	8	1	139.60	112	0.30	0.86	24.63	9.93	6.90
(6,3,1)	66	3	116.32	112	0.49	0.16	28.34	10.51	7.52
(6,3,2)	242	25	115.62	112	0.50	0.39	26.07	10.15	7.14
(6,3,3)	110	11	105.12	112	0.48	0.65	26.14	10.17	7.15
(6,3,4)	6	0	134.45	112	0.46	0.89	28.34	10.51	7.52
(6,4,1)	74	7	116.66	112	0.66	0.16	26.42	10.21	7.20
(6,4,2)	472	42	111.87	112	0.67	0.40	26.58	10.24	7.23
(6,4,3)	134	10	101.75	112	0.67	0.60	27.20	10.33	7.33
(6,4,4)	6	0	99.18	112	0.61	0.81	28.34	10.51	7.52
(6,5,1)	0	0	0.00	0	0.00	0.00	0.00	0.00	0.00
(6,5,2)	0	0	0.00	0	0.00	0.00	0.00	0.00	0.00
(6,5,3)	0	0	0.00	0	0.00	0.00	0.00	0.00	0.00
(6,5,4)	0	0	0.00	0	0.00	0.00	0.00	0.00	0.00

841
842
843

Table 18: CHOP dataset for the NonFlex scenario used in the study. Notice that CHOP groups with durations of 0 are so-called 'empty' CHOP groups, meaning that no reference operating point falls within the group boundaries. Empty CHOP-groups are discarded from the final CHOP dataset and are grey-shaded in the table.

Group (p,d,i)	t [h]	t_{PV}	c_p [€/MWh]	α_p [T/MWh]	λ_{DH}	λ_{ind}	c_{MeOH} [€/GJ]	c_{NG} [€/GJ]	c_{wood} [€/GJ]
(1,1,1)	1776	1369.3	15.34	251	0.19	0.13	21.97	9.74	6.62
(1,1,2)	1716	1230.6	15.35	241	0.18	0.35	22.55	9.82	6.70
(1,1,3)	222	130	11.85	198	0.19	0.58	24.47	10.05	6.97
(1,1,4)	0	0	0.00	0	0.00	0.00	0.00	0.00	0.00
(1,2,1)	488	350	12.77	236	0.32	0.13	22.58	9.81	6.70
(1,2,2)	1012	553	9.65	180	0.32	0.36	25.22	10.13	7.08
(1,2,3)	178	109	11.90	200	0.31	0.57	24.05	9.98	6.91
(1,2,4)	6	5	15.30	270	0.32	0.86	21.25	9.66	6.52
(1,3,1)	728	566	14.27	255	0.49	0.14	21.89	9.74	6.61
(1,3,2)	1266	815	12.39	219	0.51	0.37	23.53	9.93	6.84
(1,3,3)	576	306	8.38	175	0.50	0.57	25.52	10.17	7.12
(1,3,4)	30	18	10.57	202	0.51	0.83	24.31	10.03	6.95
(1,4,1)	434	355	14.77	263	0.67	0.16	21.50	9.69	6.55
(1,4,2)	1070	825	15.37	254	0.71	0.35	21.95	9.74	6.62

(1,4,3)	240	193	16.76	262	0.73	0.56	21.63	9.71	6.57
(1,4,4)	0	0	0.00	0	0.00	0.00	0.00	0.00	0.00
(1,5,1)	138	117	17.15	270	0.89	0.17	21.25	9.66	6.52
(1,5,2)	270	228	16.72	270	0.87	0.31	21.25	9.66	6.52
(1,5,3)	42	36	18.51	270	0.86	0.56	21.25	9.66	6.52
(1,5,4)	0	0	0.00	0	0.00	0.00	0.00	0.00	0.00
(2,1,1)	7494	5480	29.34	211	0.19	0.12	22.55	9.77	6.67
(2,1,2)	10698	8568	28.19	252	0.19	0.36	21.70	9.70	6.57
(2,1,3)	2156	1753	30.52	258	0.21	0.58	21.57	9.69	6.56
(2,1,4)	24	20	30.51	270	0.19	0.82	21.25	9.66	6.52
(2,2,1)	1824	1355	29.41	217	0.32	0.13	22.41	9.75	6.65
(2,2,2)	2852	2233	28.25	250	0.32	0.37	21.86	9.72	6.60
(2,2,3)	878	704	30.72	257	0.31	0.58	21.67	9.70	6.57
(2,2,4)	0	0	0.00	0	0.00	0.00	0.00	0.00	0.00
(2,3,1)	3380	2555	29.10	225	0.49	0.15	22.24	9.74	6.63
(2,3,2)	6508	5211	28.98	251	0.49	0.37	21.71	9.70	6.57
(2,3,3)	2748	2183	32.07	253	0.51	0.61	21.75	9.71	6.58
(2,3,4)	54	41	29.14	250	0.54	0.83	22.14	9.77	6.65
(2,4,1)	3458	2679	30.16	234	0.70	0.17	22.02	9.72	6.61
(2,4,2)	6130	4942	29.27	252	0.70	0.37	21.66	9.69	6.57
(2,4,3)	3850	3204	30.13	264	0.71	0.61	21.39	9.67	6.54
(2,4,4)	192	162	31.84	270	0.72	0.85	21.25	9.66	6.52
(2,5,1)	768	615	30.01	248	0.86	0.17	21.73	9.70	6.57
(2,5,2)	2052	1689	29.00	259	0.87	0.37	21.48	9.68	6.55
(2,5,3)	1460	1233	29.23	269	0.86	0.61	21.26	9.66	6.52
(2,5,4)	90	76	31.93	270	0.82	0.84	21.25	9.66	6.52
(3,1,1)	4584	2692	47.82	113	0.18	0.13	24.86	9.97	6.94
(3,1,2)	9290	5555	49.07	118	0.18	0.36	24.68	9.95	6.91
(3,1,3)	1464	916	49.82	138	0.21	0.58	24.17	9.90	6.85
(3,1,4)	30	20	50.80	153	0.18	0.82	23.75	9.86	6.80
(3,2,1)	1320	765	49.40	113	0.34	0.14	24.99	9.99	6.96
(3,2,2)	3060	1764	50.63	116	0.34	0.36	25.02	10.00	6.97
(3,2,3)	402	228	49.29	144	0.31	0.56	25.04	10.05	7.01
(3,2,4)	0	0	0.00	0	0.00	0.00	0.00	0.00	0.00
(3,3,1)	1916	1129	50.61	115	0.48	0.15	24.82	9.96	6.94
(3,3,2)	4006	2352	51.66	113	0.49	0.38	24.86	9.97	6.94
(3,3,3)	1294	736	51.11	121	0.52	0.59	25.13	10.02	6.99
(3,3,4)	50	30	47.20	191	0.50	0.84	24.19	9.99	6.92
(3,4,1)	1464	888	47.98	118	0.69	0.17	24.55	9.93	6.89
(3,4,2)	3534	2162	50.01	122	0.70	0.35	24.45	9.92	6.88
(3,4,3)	2268	1396	50.17	126	0.70	0.60	24.38	9.91	6.87
(3,4,4)	84	59	45.05	193	0.73	0.87	22.90	9.79	6.71
(3,5,1)	192	116	49.07	112	0.86	0.17	24.63	9.93	6.90

(3,5,2)	634	410	47.10	149	0.85	0.37	23.83	9.87	6.81
(3,5,3)	366	245	46.95	168	0.86	0.62	23.44	9.84	6.77
(3,5,4)	0	0	0.00	0	0.00	0.00	0.00	0.00	0.00
(4,1,1)	1844	869	67.87	112	0.17	0.13	27.15	10.32	7.32
(4,1,2)	6418	3424	67.02	112	0.18	0.37	25.81	10.11	7.10
(4,1,3)	1610	904	66.83	112	0.19	0.58	25.29	10.03	7.01
(4,1,4)	14	7	69.14	112	0.21	0.83	25.92	10.13	7.12
(4,2,1)	664	312	67.01	112	0.33	0.15	27.19	10.33	7.33
(4,2,2)	2232	1122	66.63	112	0.35	0.37	26.43	10.21	7.20
(4,2,3)	866	456	65.98	112	0.33	0.59	25.94	10.14	7.12
(4,2,4)	12	5	70.69	112	0.37	0.82	28.34	10.51	7.52
(4,3,1)	1326	710	64.65	112	0.49	0.15	25.77	10.11	7.09
(4,3,2)	4060	2252	66.90	112	0.48	0.38	25.42	10.05	7.03
(4,3,3)	2740	1523	67.57	112	0.49	0.62	25.39	10.05	7.03
(4,3,4)	146	76	68.14	112	0.50	0.83	26.00	10.14	7.13
(4,4,1)	1030	607	67.95	112	0.68	0.17	24.83	9.96	6.93
(4,4,2)	3016	1763	67.95	112	0.69	0.36	24.91	9.97	6.95
(4,4,3)	2472	1461	68.80	112	0.69	0.63	24.81	9.96	6.93
(4,4,4)	184	107	69.20	112	0.69	0.85	24.99	9.99	6.96
(4,5,1)	192	116	64.98	112	0.85	0.16	24.63	9.93	6.90
(4,5,2)	576	347	66.38	112	0.86	0.34	24.63	9.93	6.90
(4,5,3)	160	96	65.58	112	0.89	0.60	24.63	9.93	6.90
(4,5,4)	0	0	0.00	0	0.00	0.00	0.00	0.00	0.00
(5,1,1)	3510	1508	80.55	112	0.16	0.13	28.27	10.50	7.51
(5,1,2)	8454	3814	80.12	112	0.17	0.37	27.66	10.40	7.41
(5,1,3)	2522	1193	81.18	112	0.19	0.59	27.11	10.32	7.31
(5,1,4)	18	8	78.14	112	0.13	0.82	28.34	10.51	7.52
(5,2,1)	1326	567	79.07	112	0.34	0.14	28.34	10.51	7.52
(5,2,2)	2566	1141	79.88	112	0.34	0.38	27.84	10.43	7.44
(5,2,3)	1126	522	80.77	112	0.34	0.61	27.35	10.35	7.35
(5,2,4)	6	3	76.37	112	0.25	0.86	28.34	10.51	7.52
(5,3,1)	1628	697	81.77	112	0.51	0.17	28.31	10.51	7.52
(5,3,2)	4598	2088	80.50	112	0.50	0.38	27.59	10.39	7.39
(5,3,3)	2978	1413	79.64	112	0.51	0.62	27.07	10.31	7.31
(5,3,4)	132	61	78.73	112	0.52	0.85	27.45	10.37	7.37
(5,4,1)	692	327	80.62	112	0.67	0.17	27.13	10.32	7.32
(5,4,2)	2716	1353	79.66	112	0.69	0.38	26.53	10.23	7.22
(5,4,3)	2988	1534	79.54	112	0.69	0.63	26.21	10.18	7.16
(5,4,4)	254	144	78.60	112	0.69	0.85	25.23	10.02	7.00
(5,5,1)	0	0	0.00	0	0.00	0.00	0.00	0.00	0.00
(5,5,2)	104	63	75.71	112	0.85	0.36	24.63	9.93	6.90
(5,5,3)	0	0	0.00	0	0.00	0.00	0.00	0.00	0.00
(5,5,4)	0	0	0.00	0	0.00	0.00	0.00	0.00	0.00

(6,1,1)	642	274	100.83	112	0.17	0.12	28.34	10.51	7.52
(6,1,2)	714	322	99.31	112	0.17	0.37	27.67	10.41	7.41
(6,1,3)	254	114	106.31	112	0.19	0.59	27.71	10.41	7.42
(6,1,4)	14	7	104.16	112	0.20	0.83	25.92	10.13	7.12
(6,2,1)	342	146	112.84	112	0.31	0.13	28.34	10.51	7.52
(6,2,2)	260	112	110.90	112	0.33	0.39	28.18	10.49	7.49
(6,2,3)	136	61	114.02	112	0.33	0.60	27.75	10.42	7.42
(6,2,4)	8	5	139.60	112	0.30	0.86	24.63	9.93	6.90
(6,3,1)	702	300	109.68	112	0.55	0.16	28.34	10.51	7.52
(6,3,2)	968	436	148.36	112	0.54	0.36	27.68	10.41	7.41
(6,3,3)	530	236	176.04	112	0.52	0.61	27.81	10.43	7.43
(6,3,4)	24	10	134.73	112	0.55	0.87	28.34	10.51	7.52
(6,4,1)	698	304	179.12	112	0.67	0.17	28.10	10.47	7.48
(6,4,2)	1240	562	182.33	112	0.67	0.35	27.61	10.40	7.40
(6,4,3)	674	294	341.93	112	0.65	0.61	28.10	10.47	7.48
(6,4,4)	48	21	431.99	112	0.63	0.86	28.34	10.51	7.52
(6,5,1)	0	0	0.00	0	0.00	0.00	0.00	0.00	0.00
(6,5,2)	0	0	0.00	0	0.00	0.00	0.00	0.00	0.00
(6,5,3)	0	0	0.00	0	0.00	0.00	0.00	0.00	0.00
(6,5,4)	0	0	0.00	0	0.00	0.00	0.00	0.00	0.00